32 Li LH, Fraser TJ, Olin EJ, Bhuyan BK. Action of camptothecin on mammalian cells in culture. *Cancer Res* 1972; **32**: 2643–50.
33 Horwitz SB, Horwitz MS. Effects of camptothecin on the breakage and repair of DNA during the cell cycle. *Cancer Res* 1973; **33**: 2834–6.
34 Liu LF. Biochemistry of camptothecin. In: Milan P, Pinado H, eds. *Camptothecins: New Antitumor Agents*. Boca Raton: CRC Press, 1995; 9–19.
35 Yao R, Cooper GM. Requirement for phosphatidylinositol-3 kinase in the prevention of apoptosis by nerve growth factor. *Science* 1995; **267**: 2003–6.
36 Franke TF, Kaplan DR, Cantley LC. PI3K: downstream AKTion blocks apoptosis. *Cell* 1997; **88**: 435–7.
37 Nakashio A, Fujita N, Rokudai S, Sato S, Tsuruo T. Prevention of phosphatidylinositol 3-kinase-Akt survival signaling pathway during topotecan-induced apoptosis. *Cancer Res* 2000; **60**: 5303–9.
38 Redinbo MR, Stewart L, Kuhn P, Champoux JJ, Hol WGJ. Crystal structures of human topoisomerase I in covalent and noncovalent complexes with DNA. *Science* 1998; **279**: 1504–13.
39 Zhang HS, Cao EH, Qin JF. Homocysteine induces cell cycle G1 arrest in endothelial cells through the PI3K/Akt/FOXO signaling pathway. *Pharmacology* 2005; **74**: 57–64.
40 Yusuf I, Zhu X, Kharas MG, Chen J, Fruman DA. Optimal B-cell proliferation requires phosphoinositide 3-kinase-dependent inactivation of FOXO transcription factors. *Blood* 2004; **104**: 784–7.
41 Drolet M, Wu HY, Liu LF. Roles of DNA topoisomerases in transcription. In: Liu LF, ed. *DNA Topoisomerases: Biochemistry and Molecular Biology*. Massachusetts: Academic Press, 1994; 135–46.
42 Fujiwara H, Yamakuni T, Ueno M *et al.* IC101 induces apoptosis by Akt dephosphorylation via an inhibition of heat shock protein 90-ATP binding activity accompanied by preventing the interaction with Akt in L1210 cells. *J Pharmacol Exp Ther* 2004; **310**: 1288–95.
43 Kulp SK, Yang YT, Hung CC *et al.* 3-Phosphoinoditide-dependent protein kinase-1/Akt signaling represents a major cyclooxygenase-2-independent target for celecoxib in prostate cancer cells. *Cancer Res* 2004; **64**: 1444–51.
44 Lee TK, Man K, Ho JW *et al.* FTY720 induces apoptosis of human hepatoma cell lines through PI3-K-mediated Akt dephosphorylation. *Carcinogenesis* 2004; **25**: 2397–405.
45 Suzuki T, Kobayashi M, Isatsu K *et al.* Mechanisms involved in apoptosis of human macrophages induced by lipopolysaccharide from actinobacillus actinomycetemcomitans in the presence of cycloheximide. *Infect Immune* 2004; **72**: 1856–65.
46 Rokudai S, Fujita N, Hashimoto Y, Tsuruo T. Cleavage and inactivation of antiapoptotic Akt/PKB by caspases during apoptosis. *J Cell Physiol* 2000; **182**: 290–6.
47 Morham SG, Kluckman KD, Voulomanos N, Smithies O. Targeted disruption of the mouse topoisomerase I gene by camptothecin selection. *Mol Cell Biol* 1996; **16**: 6804–9.

 doi: 10.1111/j.1349-7006.2005.0117.x

Blockade of the Stromal Cell–Derived Factor-1/CXCR4 Axis Attenuates *In vivo* Tumor Growth by Inhibiting Angiogenesis in a Vascular Endothelial Growth Factor–Independent Manner

Bayasi Guleng,[1] Keisuke Tateishi,[1] Miki Ohta,[1] Fumihiko Kanai,[1,5] Amarsanaa Jazag,[1] Hideaki Ijichi,[1] Yasuo Tanaka,[1] Miwa Washida,[2] Keita Morikane,[6] Yasushi Fukushima,[1] Takao Yamori,[7] Takashi Tsuruo,[3] Takao Kawabe,[1] Makoto Miyagishi,[4,8] Kazunari Taira,[4,8] Masataka Sata,[2] and Masao Omata[1]

[1]Department of Gastroenterology and [2]Cardiovascular Medicine, Graduate School of Medicine, [3]Institute of Molecular and Cellular Biosciences, and [4]Department of Chemistry and Biotechnology, Graduate School of Engineering, University of Tokyo; [5]Clinical Research Center, University of Tokyo Hospital; [6]Infectious Disease Surveillance Center, National Institute of Infectious Diseases; and [7]Division of Molecular Pharmacology, Cancer Chemotherapy Center, Japanese Foundation for Cancer Research, Tokyo, Japan and [8]Gene Discovery Research Center, National Institute of Advanced Industrial Science and Technology, Tsukuba, Japan

Abstract

The interaction between the chemokine receptor CXCR4 and its specific ligand, stromal cell–derived factor-1 (SDF-1/CXCL12), mediates several cellular functions. In cancer, SDF-1-positive or CXCR4-positive cells of various lineages are detected within tumor tissues. Recent intensive research has indicated the possibility that blocking CXCR4 could reduce the metastatic potential of cancer cells. Here, we show that the inhibition of the SDF-1/CXCR4 axis decreases the growth of s.c. gastrointestinal tumors through the suppression of tumor neoangiogenesis. The neutralization of CXCR4 suppressed the growth *in vivo* of tumors derived from mouse Colon38 and PancO2 cells, whereas it did not affect the growth of Colon38 and PancO2 cells *in vitro*. This attenuation of tumor growth was found to be independent of the expression of CXCR4 by the cancer cells themselves, because CXCR4 knocked-down Colon38 cells grew similarly to control cells. Furthermore, CD31-positive tumor capillaries were reduced to 45% ($P < 0.001$) and intratumor blood flows were decreased to 65% ($P < 0.01$) by blockade of CXCR4. The vascular endothelial growth factor (VEGF) concentration in the tumors was not affected by the neutralization of CXCR4. Taken together with the detection of CXCR4-positive endothelial cells in the tumor tissues, the findings suggest that the antiangiogenic effects of the blockade of CXCR4 are related to a reduction of the establishment of tumor endothelium independently of VEGF inhibition. Our data indicate that the SDF-1/CXCR4 pathway might be a general target for anticancer strategies and that blocking this system could be cooperatively effective in combination with other antiangiogenic therapies, such as blockade of VEGF. (Cancer Res 2005; 65(13): 5864-71)

Introduction

The chemokines are a group of chemoattractant cytokines that mediate several cellular functions. Stromal cell–derived factor-1α (SDF-1) is expressed by stromal cells, including fibroblasts and endothelial cells (1, 2), and interacts specifically with the seven-transmembrane, G protein–coupled receptor CXCR4 (3). CXCR4 is expressed in various cells, such as T lymphocytes, monocytes, neutrophils (4), and endothelial cells (5, 6). On ligand binding, CXCR4 activates several signaling cascades, including the phosphatidylinostiol 3-kinase and mitogen-activated protein kinase cascades, which induce cytoskeletal rearrangement, antiapoptosis effects, and cell growth (7). Importantly, the SDF-1/CXCR4 interaction is critical for the homing and retention of hematopoietic stem cells within the bone marrow and is essential in fetal hematopoiesis (8).

Recently, intensive research has indicated that CXCR4 is involved in increasing the metastatic potential of colon and breast cancer cells (2, 9, 10). For example, *CXCR4* was one of the few genes that was up-regulated in bone-metastasized breast cancer cells (11), and cells that had metastasized to the lungs expressed very high levels of CXCR4 compared with the parental tumor cells. Another study found that SDF-1 was up-regulated in malignant tissues (12). *In vivo*, neutralizing the interaction of CXCR4 and SDF-1 significantly impaired the metastasis of breast cancer cells and cell migration (2). These findings suggest the possibility that inhibition of the SDF-1/CXCR4 axis could be a strategy for the prevention of cancer cell metastasis. The mechanism by which CXCR4 expression enhances tumor metastasis is still unclear; however, the activation of CXCR4 by SDF-1 seems to have the ability to trigger the adhesion of a variety of tumor cell lines to extracellular matrix substrates, such as fibronectin (13, 14), and to vascular endothelial cells by increasing the vascular permeability (12, 15).

Tumor neovascularization, a rate-limiting step in cancer progression, is thought to be established by the sprouting of blood vessels through the division of differentiated endothelial cells. However, the growth of new vessels can be mediated in several ways. Recently, circulating endothelial progenitor cells mobilized from the bone marrow were detected in the peripheral blood of several species and were implicated in the neoangiogenesis involved in tumorigenesis as well as in the formation of new vessels after trauma, burn injury, and myocardial infarction (16–18). The SDF-1/CXCR4 axis mediates the guidance of primordial stem cells to sites of rapid vascular expansion during embryonic organogenesis (19). An analysis of CXCR4-deficient mice revealed that the receptor was essential for fetal gastrointestinal vascular formation (20), suggesting a pivotal role of the SDF-1/CXCR4 axis in fetal angiogenesis (8). Like embryonic vasculogenesis, tumor angiogenesis might be mediated by various progenitor cells

Requests for reprints: Keisuke Tateishi, Department of Gastroenterology, Graduate School of Medicine, University of Tokyo, 7-3-1 Hongo, Bunkyo-ku, Tokyo 113-8655, Japan. Phone: 81-3-3815-5411, ext. 30237; Fax: 81-3-3814-0021; E-mail: tateishik-int@h.u-tokyo.ac.jp.

(21). We analyzed the contribution of the SDF-1/CXCR4 interaction to tumor neoangiogenesis using a mouse model. Here, we show that the *in vivo* neutralization of CXCR4 also results in the attenuation of tumor growth by the inhibition of tumor neovascularization in a vascular endothelial growth factor (VEGF)–independent manner regardless of whether the cancer cells express CXCR4. CXCR4-targeting therapy might be applied as an antiangiogenic strategy for treatment of a broad spectrum of cancers.

Materials and Methods

Animals and cells. All C57BL/6 mice and BALB/c nude mice were purchased from Clea Corp. (Tokyo, Japan). The transgenic mice (C57BL/6 background) that ubiquitously expressed enhanced green fluorescent protein (GFP mice) were a generous gift from Dr. Masaru Okabe (Osaka University, Osaka, Japan; ref. 22). All procedures involving experimental animals were done in accordance with protocols approved by the Institutional Committee for Animal Research of the University of Tokyo and complied with the USPHS *Policy on Humane Care and Use of Laboratory Animals*. Colon38 (23) and PancO2 (24) cells are colon and pancreatic cancer cells, respectively, derived from C57BL/6 mice. PancO2 cells were obtained from Dr. Michael A. Hollingsworth (Eppley Institute, University of Nebraska, Omaha, NE).

Stable knockdown of CXCR4. A plasmid carrying RNA interference targeted to mouse CXCR4 was constructed as described previously (25, 26). The siCXCR4 sequence of the mouse *CXCR4* gene (5′-GCAAAGACTTATA-TAATATAT-3′) was selected using our original algorithm. Colon38 cells were transfected with pcPUR+U6-siCXCR4 or pcPUR+U6-siRenilla (control) and selected as puromycin-resistant pools. Then, quantitative reverse transcription-PCR (RT-PCR) was done to confirm the CXCR4 mRNA suppression using the primers 5′-TCAGCCTGGACCGGTACCT-3′ and 5′-GCAGTTTCC-TTGGCCTTTGA-3′.

Bone marrow transplantation and tumor implantation model. The bone marrow of lethally irradiated C57BL/6 mice was reconstituted by transplantation with bone marrow cells from GFP mice (GFP-BMT mice). Briefly, wild-type C57BL/6 mice were lethally irradiated with a total dose of 950 rads (MBR-1520RB, Hitachi, Tokyo, Japan; ref. 27); then, 2×10^6 bone marrow cells from GFP mice were injected into the tail veins of the irradiated recipient mice. The bone marrow cells of the GFP-BMT mice were sampled at 4 weeks after bone marrow transplantation, and the degree of chimerism was investigated by flow cytometry (EPICS XL, Beckman Coulter, Fullerton, CA). More than 85% of the cells in the recipient bone marrow were GFP positive using these experimental conditions (data not shown). Tumors were induced by s.c. injection of 2×10^6 cancer cells into the flank >4 weeks after the bone marrow transplantation. Large tumors were typically observed by 4 weeks after tumor implantation. The mice were anesthetized with pentobarbital sodium (120 mg/kg), and the tumor tissues were harvested for histologic analysis.

Isolation of tumor-infiltrating cells and reverse transcription-PCR analysis. Tumor-infiltrating cells (TIC) were isolated from the tumors formed by Colon38 and PancO2 cells using density gradient centrifugation in Percoll/RediGrad (Amersham Biosciences, Buckinghamshire, United Kingdom) as described previously (28). The total RNA was extracted from the TICs using ISOGEN reagent (Nippon Gene Co., Tokyo, Japan), and the reverse transcription reaction and PCR amplification were done as described (29). The PCR primer sequences were as follows: sense 5′-GGCTGTAGAGCGAGTGTTGC-3′ and antisense 5′-GTAGAGGTTGA-CAGTGTAGAT-3′ for CXCR4 (29) and sense 5′-GTTGGATACAGGCCA-GACTTTGTTG-3′ and antisense 5′-GATTCAACTTGCGCTCATCTTAGGC-3′ for hypoxanthine phosphoribosyltransferase (HPRT).

Immunohistochemistry. Tumor tissue samples were fixed in 2% paraformaldehyde and embedded with a Technovit catalyst system (Heraeus Kulzer GmbH & Co. KG, Wehrheim, Germany; ref. 30). The primary antibodies were as follows: rabbit anti-rat CXCR4 (Torrey Pines Biolabs, Inc., Houston, TX), rabbit anti-mouse CXCR4 (H-118) and anti-VEGF (sc-507; Santa Cruz Biotechnology, Santa Cruz, CA), rabbit anti-mouse SDF-1α (Torrey Pines Biolabs), rat anti-mouse CD31 (BD PharMingen, San Diego, CA), and rat anti-mouse Mac3 (BD PharMingen). The secondary antibodies were conjugated with fluorochrome Alexa Fluor 488 or 555 (Molecular Probes, Inc., Eugene, OR). The sections were observed under a confocal microscope (Leica Microsystems, Wetzlar, Germany; ref. 31).

***In vivo* neutralizing antibody studies.** Cancer cells (Colon38 or PancO2; 8×10^6) were s.c. injected into BALB/c nude mice. One group of tumor-bearing mice ($n = 5$) then received an i.p. injection of 10 μg rabbit anti-rat CXCR4-neutralizing antibody, which is reported to also bind to murine CXCR4 (32). The control group of tumor-bearing mice received 10 μg normal rabbit IgG. The mice were treated every 24 hours starting on day 3 for a total of eight separate injections of anti-CXCR4 antibody. The tumor size was measured, and the volume was calculated as [length (mm) × width $(mm)^2$] / 2. The experiments were also done using C57BL/6 mice ($n = 4$).

3-(4,5-Dimethylthiazol-2-yl)-2,5-diphenyltetrazolium bromide assay. The direct effect of the neutralizing antibody on the viability of the tumor cells was assessed by seeding 3×10^4 Colon38 cells in 24-well microplates and replacing the medium with medium containing 10 μg/mL normal IgG or 10 μg/mL anti-CXCR4-neutralizing antibody ($n = 3$) after 24 hours. The number of viable cells was determined using the 3-(4,5-dimethylthiazol-2-yl)-2,5-diphenyltetrazolium bromide (MTT) assay (Sigma, St. Louis, MO) at 24, 48, and 72 hours (33). Similarly, a total of 3×10^4 Colon38-siCXCR4 or Colon38-siRenilla cells were cultured with 300 ng/mL recombinant human SDF-1α (PeproTech EC, London, United Kingdom) in 24-well microplates, and the number of viable cells was analyzed using the MTT assay at 24, 48, and 72 hours.

Fluorescent phalloidin staining. A total of 10^5 Colon38 or PancO2 cells were seeded in two-well chambers and incubated with 10 μg/mL normal IgG or 10 μg/mL anti-CXCR4-neutralizing antibody with 300 ng/mL recombinant human SDF-1α for 24 hours; then, the cells were stained with Alexa Fluor 488–labeled phalloidin according to the manufacturer's instructions.

Cell migration assay (wound closure assay). A total of 10^5 Colon38 or PancO2 cells were seeded in two-well chambers, and confluent cell monolayers were wounded by scraping using a pipette tip of the same width and replacing the medium with medium containing 10 μg/mL normal IgG or 10 μg/mL anti-CXCR4-neutralizing antibody with 300 ng/mL recombinant human SDF-1α for 24 hours. Then, the cells were fixed and stained with Diff-Quick, and cell migration was observed using bright-field microscopy at ×40 magnification.

Quantitative reverse transcription-PCR. A total of 5×10^5 Colon38 or PancO2 cells were seeded in 6-cm dishes and incubated with 10 μg/mL normal IgG or 10 μg/mL anti-CXCR4-neutralizing antibody for 24 hours. The total RNA was extracted, treated with DNase, and purified. Quantitative RT-PCR analysis was done using an ABI 7000 Real-time PCR System (Applied Biosystems, Foster City, CA). The mRNA level of each gene was normalized to HPRT. The primers were as follows: basic fibroblast growth factor (bFGF), forward 5′-CACCAGGCCACTTCAAGGA-3′ and reverse 5′-GATGGATGCGCAGGAAGAA-3′; platelet-derived growth factor (PDGF), forward 5′-AAGCTCGGGTGACCATTCG-3′ and reverse 5′-ACTTT-CGGTGCTTGCCTTTG-3′; and placenta growth factor (PlGF), forward 5′-CCCTGTCTGCTGGGAACAA-3′ and reverse 5′-GCTGCGACCCCA-CACTTC-3′. The SDF-1, matrix metalloproteinase-9 (MMP-9), intercellular adhesion molecule (ICAM), and VCAM (VCAM) primer sequences were reported previously (34).

Late-outgrowth endothelial colony assay. To isolate the peripheral blood mononuclear cells (PBMC; ref. 18), blood samples (500-1,000 μL) from mice were collected in heparinized tubes ~3 weeks after tumor implantation. The PBMCs were isolated by Ficoll gradient centrifugation (Amersham Biosciences AB, Uppsala, Sweden). To detect circulating endothelial cells, 3×10^5 freshly isolated PBMCs were cultured in modified endothelial growth medium (EGM), which was composed of X-vivo-20 serum-free medium with VEGF (10 ng/mL, R&D, Minneapolis, MN), endothelial cell growth supplement (30 μg/mL, Upstate, Lake Placid, NY), human recombinant bFGF (5 ng/mL, Invitrogen, Carlsbad, CA), heparin

(5 units/mL), streptomycin (100 μg/mL), penicillin (100 units/mL), and fungizone (0.25 μg/mL). The PBMCs were placed in two-well chambers coated with 0.2% gelatin (17, 18) and incubated at 37°C in a humidified environment with a 5% CO_2 atmosphere. Monocytes and mature endothelial colonies attached to the well chambers within 3 days. The nonadherent cells were transferred to other wells in EGM after 3 days. After 2 weeks, the endothelial colonies were characterized by the metabolic uptake of acetylated low-density lipoprotein labeled with 1,1′-dioctadecyl-3,3,3′,3′-tetramethylindocarbocyanine perchlorate (DiI-Ac-LDL; Biomedical Technologies, Stoughton, MA). The cells were incubated with 10 μg/mL DiI-Ac-LDL at 37°C for 4 hours and examined by fluorescence microscopy. DiI-Ac-LDL and GFP double-positive colonies that formed at 2 weeks were considered late-outgrowth colonies (17).

Measurement of local blood perfusion in superficial tumor tissue. The blood perfusion of the tumors was measured using a laser Doppler perfusion imaging (LDPI) system (Moor Instruments, Devon, United Kingdom; refs. 35, 36). The LDPI data were acquired from mice on day 10 following five antibody treatments given at 24-hour intervals. Each mouse was anesthetized 15 minutes before the recordings to eliminate artifacts caused by body movements; the mouse was placed on a heating plate at 40°C, and the LDPI recording was made (35, 36).

Estimation of vascular endothelial growth factor levels in subcutaneuse tumors and cultured supernatants. The tumor tissues were harvested on day 14 after five antibody treatments and homogenized with a tissue homogenizer in 9 volumes of lysis buffer [300 mmol/L NaCl, 15 mmol/L Tris-HCl, 2 mmol/L $MgCl_2$, 2 mmol/L Triton X-100, 20 ng/mL pepstatin A, 20 ng/mL leupeptin, 20 ng/mL aprotinin (pH 7.4)]. A total of 3×10^5 Colon38 or PancO2 cells were seeded in six-well plates and incubated with fetal bovine serum–free medium containing 10 μg/mL normal IgG or 10 μg/mL anti-CXCR4-neutralizing antibody for 24 hours. The ELISA assay for VEGF was done by the SRL analysis service (Tokyo, Japan).

Statistical analysis. The data are expressed as mean ± SE. Comparisons between the groups were analyzed using Student's t test. $P < 0.05$ was considered statistically significant.

Results

CXCR4-positive cells contribute to the establishment of tumor tissues in a cancer cell type–independent manner. To estimate the role of the SDF-1/CXCR4 axis in the establishment of gastrointestinal tumors, in addition to its known metastasis-promoting ability, we analyzed two models of s.c. tumors in mice using two mouse-derived cancer cells, Colon38 and PancO2. CXCR4 mRNA was not detected in cultured PancO2 cells but was detected in Colon38 cells (Fig. 1*A*). However, CXCR4-positive cells were detected in the tissues of tumors established from implanted Colon38 and PancO2 cells; the CXCR4-positive cells were observed around the tumor vessels and occasionally in the endothelium (Fig. 1*B, arrow*). These findings suggested that the cells infiltrating the tumor might express CXCR4 regardless of whether the cancerous cells themselves express CXCR4. To clearly distinguish cancer cells from TICs, we established a mouse model in which the bone marrow was depleted by irradiation and then reconstituted by transplantation of GFP-tagged bone marrow cells (GFP-BMT mice). Many bone marrow–derived cells were found to infiltrate into both types of tumor tissues, and GFP and CXCR4 double-positive cells were detected around the tumor vessels (Fig. 1*C, arrow*). To confirm the expression of CXCR4 in the TICs, TICs were isolated from tumor tissues as described previously, and the expression levels of various chemokine receptors were analyzed by RT-PCR (data not shown). CXCR4 mRNA was detected in the TICs of both Colon38 and PancO2 tumors (Fig. 1*A*). To investigate the percentage of CXCR4-expressing cells in bone marrow–derived cells, we counted the total numbers of GFP and CXCR4 double-positive cells as the

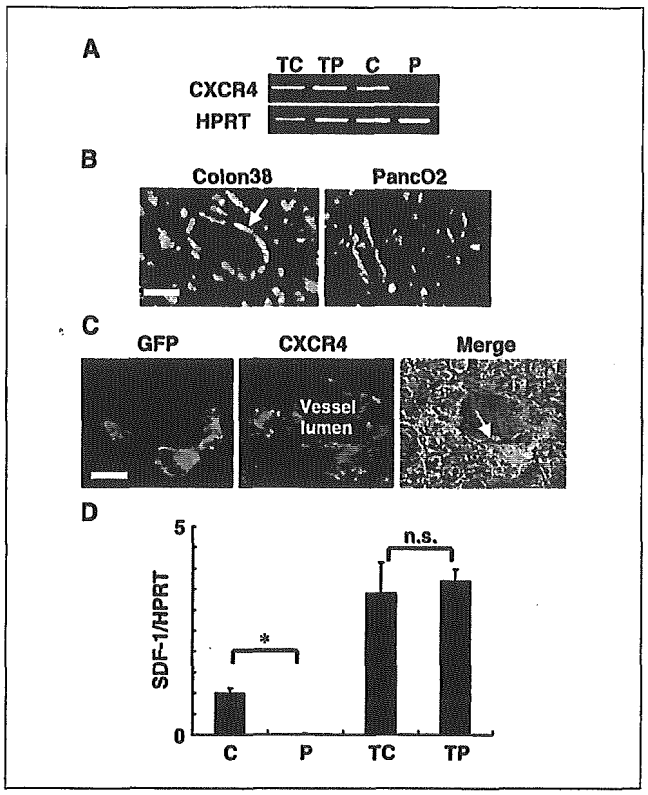

Figure 1. CXCR4-positive cells in s.c. colon and pancreatic tumor tissues. *A*, expression of CXCR4 mRNA was commonly detected by RT-PCR in TICs and in cultured Colon38 cells but not in cultured PancO2 cells. *TC*, TICs from Colon38 tumors; *TP*, TICs from PancO2 tumors; *C*, cultured Colon38 cells; *P*, cultured PancO2 cells. *B*, Colon38 (*left*) and PancO2 (*right*) tumor tissues were stained with anti-CXCR4 (*green*) and anti-CD31 (*red*) antibodies. CXCR4-positive cells were observed around the tumor vessels, and some lined the endothelium (*arrow*). *Bar*, 20 μm. *C*, Colon38 tumor tissues from GFP-BMT mice were stained with anti-CXCR4 antibody. GFP and CXCR4 double-positive cells were found around the tumor vessels (*right, arrow*). *Right*, merged image of differential interference contrast images, GFP (*green*) and CXCR4 (*red*). *Bar*, 20 μm. *D*, total RNA was isolated from s.c. tissues and the two cell lines, and the expression of SDF-1 was analyzed by quantitative RT-PCR.

number per square millimeter using fluorescence microscopy ($n = 3$). GFP and CXCR4 double-positive cells constituted ~3.4% (32.3 ± 2.1 versus 961.3 ± 36.8) or 2.1% (65.7 ± 4.6 versus 3185.7 ± 149.8) of all bone marrow–derived cells in Colon38-derived or PancO2-derived tumors, respectively. For a while, SDF-1 was detected in the extracellular portion of the stromal area, especially around the vessels in both Colon38-derived and PancO2-derived tumors (data not shown). To quantify the expression of SDF-1, we extracted total RNA from s.c. tissues and the two cell lines and did quantitative RT-PCR (Fig. 1*D*). The expression of SDF-1 was induced in both tumor tissues. PancO2 cells did not express SDF-1 *in vitro*; nevertheless, the level of SDF-1 expression in s.c. tumors was not very different from that in Colon38. These findings suggest that SDF-1 is secreted from noncancerous tissues in the tumors or expression could be up-regulated in the tumor tissues. Therefore, the SDF-1/CXCR4 axis seems to contribute to the establishment of tumor tissues via the expression of CXCR4 on infiltrating cells regardless of whether the cancer cells themselves express CXCR4.

CXCR4 neutralization prevents the growth of Colon38 and PancO2 tumors regardless of CXCR4 expression by the cancer cells. We evaluated the therapeutic potential of the neutralization

of CXCR4 for the inhibition of tumor formation using the tumor transplant model. To interfere with SDF-1/CXCR4 signaling, BALB/c nude mice transplanted with Colon38 and PancO2 cells were treated with anti-CXCR4-neutralizing antibody or a control antibody using the dose schedule described in a previous report (32). The growth of Colon38 xenograft tumors was clearly suppressed in the group treated with the neutralizing antibody compared with the control group (n = 5; Fig. 2*A*). Neutralizing antibody against CXCR4 also suppressed the growth of PancO2 tumors (n = 5; Fig. 2*B*). This finding was reproduced in the experiment using C57BL/6 mice. As shown in Fig. 2*C*, neutralizing antibody against CXCR4 also suppressed the growth of Colon38 tumors in C57BL/6 mice (n = 4). As Colon38 cells had been shown to express CXCR4 (Fig. 1*A*), we examined whether the anti-CXCR4-neutralizing antibody could directly inhibit their growth. Colon38 cells were cultured in the presence of 10 μg/mL anti-CXCR4 antibody or control antibody to simulate the concentration in the peripheral blood of treated mice. Under these *in vitro* conditions, anti-CXCR4 antibody treatment had no effect on the growth of Colon38 cells (n = 3; P = 0.93; Fig. 2*D*). To confirm that the effect was independent of the CXCR4 expression by cancer cells themselves, we established Colon38-siCXCR4 cells in which the *CXCR4* gene was stably suppressed. As shown in Fig. 2*E*, the siCXCR4 effectively blocked CXCR4 mRNA expression. Colon38-siCXCR4 cells or Colon38-siRenilla cells were transplanted s.c. into mice and the difference in growth rates was compared. As shown in Fig. 2*G*, growth rates were not significantly different between the two groups (n = 5; P > 0.1). Growth rates were also similar in the *in vitro* culture experiments (Fig. 2*F*).

In addition, we investigated whether the neutralizing antibody has other biological effects *in vitro*, because the SDF-1/CXCR4 axis is significant in breast and colon cancer metastasis. Obvious cytoskeletal changes were not detected by fluorescent phalloidin staining of groups of the two cell lines stained with anti-CXCR4

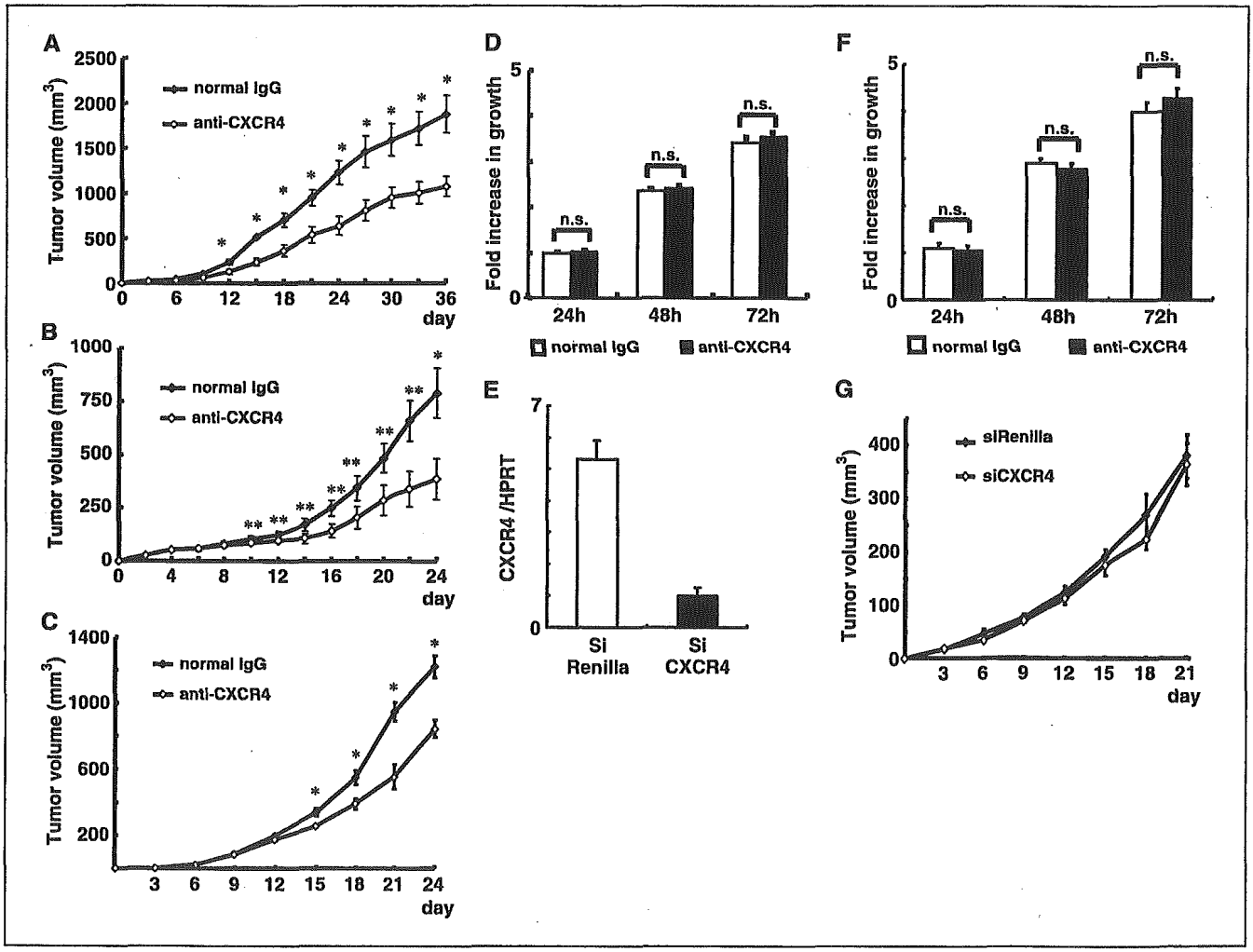

Figure 2. CXCR4 neutralization blocked the growth of s.c. tumors derived from Colon38 and Panco2 cells. BALB/c nude mice were s.c. inoculated with 8 × 10^6 tumor cells. Mice were injected i.p. with anti-CXCR4-neutralizing antibody (10 μg/injection) or with control normal IgG (10 μg/injection) every 24 hours for a total of eight separate injections. Neutralizing antibody against CXCR4 suppressed the growth of tumors derived from Colon38 (*A*) and PancO2 (*B*) cells (n = 5). *Points*, mean; *bars*, SE. *, P < 0.05; **, P < 0.005 (Student's t test). *C*, neutralizing antibody against CXCR4 also suppressed the growth of Colon38 tumors in C57BL/6 mice (n = 4). *D*, anti-CXCR4 antibody treatment had no effect on the growth of cultured Colon38 cells (n = 3; P = 0.93). *n.s.*, not significant. *E*, Colon38 cells were stably transfected with pcPUR+U6-siCXCR4 or pcPUR+U6-siRenilla (control); then, quantitative RT-PCR was done to confirm the CXCR4 mRNA suppression. *F*, growth rates of Colon38-siCXCR4 or Colon38-siRenilla cells were also similar in the *in vitro* culture experiments. *G*, Colon38-siCXCR4 and Colon38-siRenilla cells were transplanted s.c. and the difference in their growth rates was compared (n = 5). *Points*, mean; *bars*, SE.

antibody and control antibody (data not shown). To examine whether the anti-CXCR4-neutralizing antibody treatment affects cell migration, we did a cell migration assay (wound closure assay). No difference in cell migration was observed between the groups for either cell line (data not shown). Between the two groups for both cell lines, there was no statistical difference in the mRNA expression of ICAM (n = 4; P > 0.1), VCAM (n = 4; P > 0.1), PDGF (n = 4; P > 0.1), PlGF (n = 4; P > 0.1), bFGF (n = 4; P > 0.1), or MMP-9 (n = 4; P > 0.1). The VEGF secretion of the Panco2 cells *in vitro* was not statistically different between the two groups (n = 4; P = 0.92). VEGF production was not detected in the Colon38 cell line. These findings indicate that the suppression of tumor growth was not mediated by the direct inhibition of cancer cell growth.

CXCR4 neutralization decreases the development of tumor endothelium *in vivo*. As CXCR4-positive cells were detected among endothelial cells as well as in the perivascular area (Fig. 1*B*), the effect of CXCR4 neutralization on tumor angiogenesis was estimated by histologic examination of tumors for CD31, an endothelial marker (Fig. 3*A*). The capillary density was calculated as the number of capillaries per square millimeter exhibiting expression of CD31 based on counts in 10 randomly selected fields from each tissue preparation examined by confocal microscopy. Staining with anti-CD31 antibody showed that the density of vessels in the tumors of the mice treated with the neutralizing antibody was significantly lower than that in the tumors of the control group (n = 3; P = 0.00048; Fig. 3*B*). In addition, the Colon38-siCXCR4 or Colon38-siRenilla cells were transplanted into mice s.c.

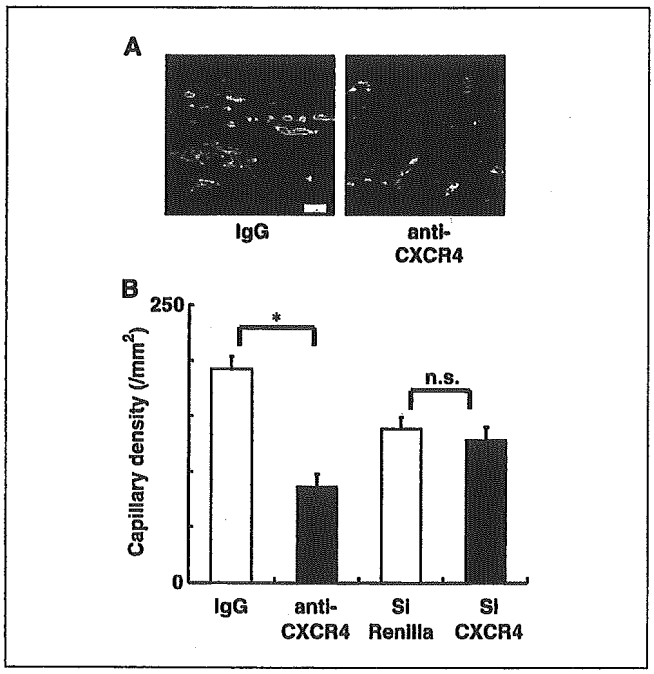

Figure 3. CXCR4 neutralization decreased tumor vessel densities. C57BL/6 mice were injected s.c. with 2 × 10^6 Colon38 cells. After 1 week, the mice (n = 3) were injected i.p. with 10 μg anti-CXCR4-neutralizing antibody or 10 μg normal rabbit IgG (control group). *A*, representative images of CD31 immunostaining after a total of five separate antibody injections. *Bar*, 50 μm. *B*, capillary density was calculated as the number of capillaries per square millimeter based on the counts of 10 randomly selected fields. Treatment with anti-CXCR4 antibody decreased tumor vessel densities (*right*) compared with the control group (*left*). *Columns*, mean (n = 3); *bars*, SE. *, P < 0.05 (Student's t test). The capillary densities in the tumors derived from Colon38-siCXCR4 cells or Colon38-siRenilla cells were not significantly different (n = 3; P = 0.51).

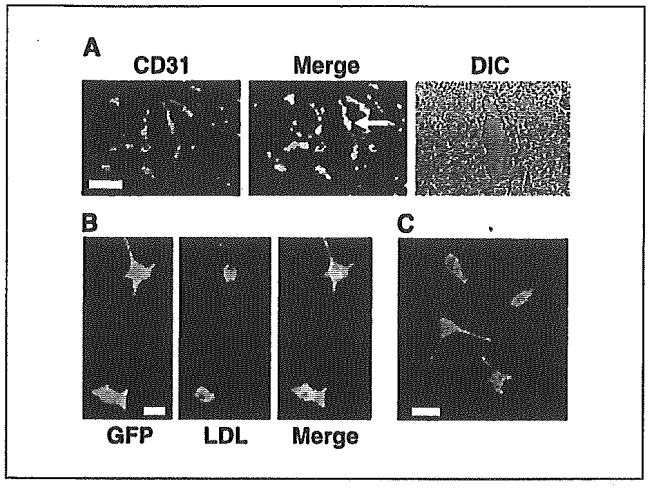

Figure 4. Bone marrow–derived endothelial cells were analyzed *ex vivo* and *in vivo*. *A*, histologic sections of Colon38 tumors from GFP-BMT mice were stained with anti-CD31 antibody (*red*) to detect bone marrow–derived endothelial cells. GFP-positive cells (*green*) rimmed by CD31-positive margins are seen in the tumor endothelium (*arrow*). *Bar*, 20 μm. *B*, PBMCs were analyzed using the late-outgrowth endothelial colony assay. Endothelial cells positive for both DiI-Ac-LDL (*LDL*; *red*) and GFP (*green*) were detected in peripheral blood. *Bar*, 10 μm. *C*, late-outgrowth endothelial cells expressed CXCR4 (*red*). *Bar*, 20 μm.

and the vascularity of the tumors was compared. The capillary densities in the tumors in the two groups were not significantly different (n = 3; P = 0.51; Fig. 3*B*). Recently, bone marrow–derived endothelial cells were reported to be involved in tumor angiogenesis in tumor implantation models (16–18, 37). To investigate whether bone marrow–derived endothelial cells formed the tumor vessel endothelium in our model, the expression of GFP in the endothelium of the tumor xenografts in GFP-BMT mice was analyzed. GFP and CD31 double-positive cells were observed lining the vessels only in rare instances, suggesting that the population of bone marrow–derived tumor endothelial cells was very limited in our model (Fig. 4*A*). The presence of endothelial progenitor cells in the peripheral blood of tumor-bearing mice was investigated using the late-outgrowth assay. PBMCs were cultured to permit the growth of endothelial colonies, which were then identified by the metabolic uptake of DiI-Ac-LDL after 2 weeks of culture. The expression of GFP was detected in most of the DiI-Ac-LDL-positive colonies (Fig. 4*B*), but these cells did not form large colonies under our experimental conditions. Importantly, late-outgrowth cells identified *in vitro* expressed the chemokine receptor CXCR4 (Fig. 4*C*).

***In vivo* neutralization of CXCR4 decreases the intratumor blood flow.** As the blockade of CXCR4 induced a decrease in the development of intratumor endothelial cells, we monitored dynamic changes in the blood perfusion of the tumors using a LDPI system (35, 36). LDPI can provide noninvasive analysis of local perfusion in superficial tissues. The technique is based on the principle that the wavelength of laser light changes (Doppler shift) when it is reflected from a moving object (RBC in this case), whereas the wavelength of light reflected from a stationary object remains unchanged. The Doppler-shifted light is converted into an arbitrary perfusion signal, which is approximately proportional to the mean blood cell velocity multiplied by the concentration of moving blood cells (Fig. 5*A*). The blood flow in the tumors treated with neutralizing antibody was decreased to ~65% of that in the control tumors for both s.c. Colon38 and PancO2 tumors (n = 7; P < 0.01 and

$P < 0.001$, respectively; Fig. 5*B*). Taken together with the observations presented in Fig. 2, these findings indicate that neutralization of CXCR4 suppresses tumor growth by an antiangiogenic mechanism and not by direct inhibition of cell growth. In addition, the Colon38-siCXCR4 or Colon38-siRenilla cells were transplanted into mice s.c. The Doppler flow rates in the tumors were similar ($n = 5$; $P = 0.57$; Fig. 5*B*). These results indicate that the decrease in tumor vascularity with anti-CXCR4 neutralizing antibodies is not caused by a direct effect against cancer cells.

CXCR4 neutralization did not change vascular endothelial growth factor expression in the tumor tissues or induce critical anemia. Cells of inflammatory cell lineages that infiltrate into tumors have been reported to secrete VEGF, a pivotal angiogenic factor (38, 39). By immunohistochemistry, some of the infiltrated cells were Mac3 positive, which indicated that monocytes/macrophages had been recruited into the tumor tissues from the bone marrow (Fig. 6*A*). In a short time, few anti–smooth muscle actin–positive cells were detected in our analysis (data not shown), which might be consistent with reports that tumor microvessels often lack a lining of smooth muscle cells unlike normal vessels. To determine whether the TICs secrete VEGF in our xenograft tumor model, we counterstained the GFP-positive cells of Colon38 tumor with anti-VEGF antibody. As shown in Fig. 6*B*, VEGF was expressed in the GFP-positive, bone marrow–derived infiltrating cells in our xenograft tumors (Fig. 6*B*). To clarify the effect of blocking CXCR4 on VEGF expression, the VEGF concentrations in the tumors were determined using ELISA and compared between the groups treated with CXCR4-neutralizing antibody and control antibodies. As shown in Fig. 6*C*, the VEGF concentration was not significantly affected by CXCR4 neutralization. These findings suggest that the suppression of angiogenesis by the neutralization of CXCR4 is not attributable to a change in the VEGF concentration and that VEGF secretion does not always depend on CXCR4-positive TICs. Indeed, the blockade of CXCR4 did not cause a major change in the number of perivascular bone marrow–derived GFP-positive cells in the tumor tissues (Fig. 6*D*). Inflammatory cells that infiltrate tumors have been reported to express various angiogenic factors. It has been suggested that the cells producing vascular mitogens can be mobilized by other mechanisms independent of SDF-1/CXCR4 signaling. Furthermore, because the SDF-1/CXCR4 axis is indispensable for hematopoietic stem cell homing (8), the inhibition of this interaction might impair bone marrow hematopoiesis. To exclude the possibility that the decrease in tumor perfusion measured in mice treated with CXCR4-neutralizing antibody was caused by anemia, which can result in the underestimation of intratumor blood flow by the LDPI system, the peripheral blood cell counts were determined for each

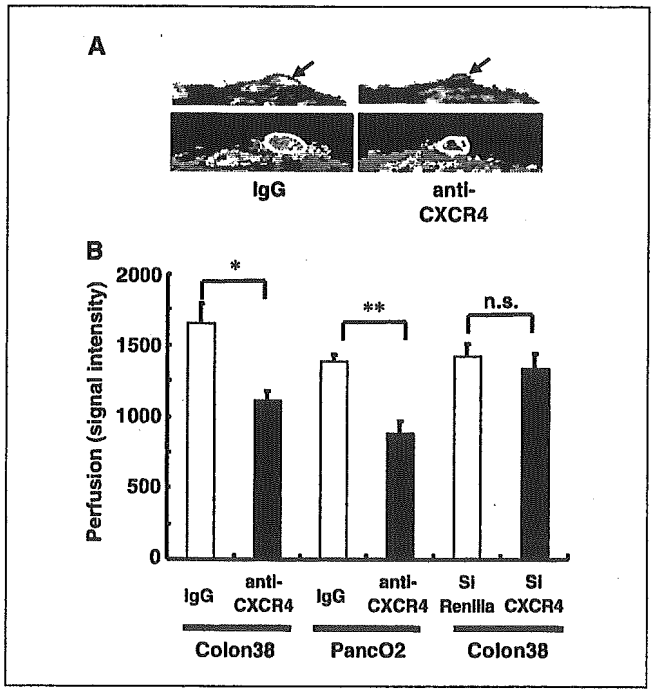

Figure 5. CXCR4 neutralization decreased the intratumor blood flow *in vivo*. *A*, representative images of blood flow in tumor tissues from the LDPI system. *Arrow*, s.c. tumor (*top*). The average flow in closed areas was measured as the intratumor blood flow (*bottom*). *B*, blood flow in s.c. Colon38 and PancO2 tumors treated with CXCR4-neutralizing antibody was decreased in comparison with the control tumors ($n = 7$). *, $P < 0.01$; **, $P < 0.001$. The blood flow in s.c. Colon38-siCXCR4-derived or Colon38-siRenilla-derived tumors was also estimated ($n = 5$; $P > 0.5$).

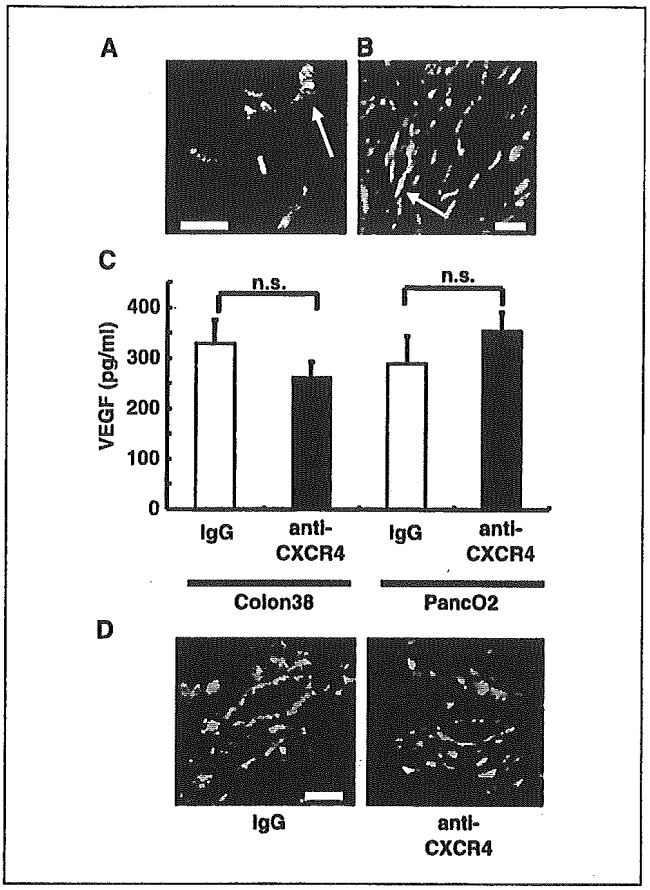

Figure 6. Neutralization of CXCR4 did not change the VEGF concentration in the Colon38 and PancO2 tumors. *A*, Colon38 tumor tissue of GFP-BMT mice was immunostained with anti-Mac3 antibody. Some of the GFP-positive infiltrating cells were Mac3 positive (*arrow*). *Bar*, 10 μm. *B*, Colon38 tumor of GFP-BMT mice was counterstained with anti-VEGF antibody. VEGF expression (*red*) was seen in the GFP-positive, bone marrow–derived infiltrating cells in our xenograft tumors (*arrow*), *Bar*, 10 μm. *C*, concentration of VEGF was determined by ELISA assay in the tumors on day 14 following five antibody injections and was compared between the groups treated with anti-CXCR4-neutralizing antibody and with control antibodies ($n = 7$). *D*, no major change in the number of perivascular bone marrow–derived GFP-positive cells in the tumor tissues treated with CXCR4 blockade compared with control tumors. *Red*, CD31-positive endothelial cells. *Bar*, 20 μm.

group (Table 1). The peripheral blood cell counts were not significantly different between the groups, which indicated that CXCR4 antibody did not induce a critical suppression of the bone marrow under our experimental conditions.

Discussion

In this study, we showed that the SDF-1/CXCR4 axis, which is indispensable for hematopoiesis and angiogenesis in the embryo (20, 40), plays a pivotal role in tumor progression through promoting tumor neovascularization. Our findings might provide new insight on the significance of the SDF-1/CXCR4 axis in local tumor progression. The reported ability of CXCR4 neutralization to block the growth of metastatic lesions might be mediated in part by this inhibition of angiogenesis. Although this antigrowth effect is independent of CXCR4 expression by cancer cells, based on the results of small interfering RNA experiments, this does not contradict the recent reports that *in vivo* breast cancer growth was dependent on CXCR4 (41). The significance of the SDF-1/CXCR4 axis for cancer cell growth *in vivo* could differ by cancer cell type. For example, the CXCR4 expression of gastrointestinal tumors might be less than that of breast cancer. In addition, another mitogenic signaling pathway could compensate for the growth disadvantage by inhibiting the SDF-1/CXCR4 axis in gastrointestinal tumors. Indeed, oncogenic mutations of the *K-Ras* or *B-Raf* genes that strongly induce hyperproliferative capacity are often reported in gastrointestinal tumors. Importantly, the anticancer potential of the CXCR4-blocking strategy may be effective for a broad spectrum of cancers.

During tumor progression, infiltrating cells produce several potent angiogenic growth factors, cytokines, and proteases (38, 39). The recruitment and infiltration of circulating cells are mediated by members of the chemokine family of chemoattractive cytokines. In our murine tumor models, the neutralization of CXCR4 did not change the concentration of VEGF in the tumors, suggesting that other chemokine systems function in the recruitment of VEGF-secreting cells. Although the capillary density was lower in anti-CXCR4-treated tumors in spite of unchanged VEGF concentrations, our data do not exclude the significance of VEGF in tumor angiogenesis. Our results indicate that the SDF-1/CXCR4 axis does not always regulate tumor angiogenesis in a VEGF-dependent manner; for example, the SDF-1/CXCR4 axis might contribute to functional vascular establishment by the regulation of endothelial tube formation (1).

Recently, circulating endothelial progenitor cells mobilized from bone marrow have been detected in the peripheral blood of several species and shown to be involved in neoangiogenesis in tumors as well as in the formation of new vessels after trauma, burn injury, and myocardial infarction (16–18). We have already documented the roles of bone marrow–derived vascular progenitor cells in vascular remodeling using the original reconstituted bone marrow mouse model (27, 30). In the present study using Colon38 and Panco2 cells, bone marrow–derived endothelial cells were infrequently detected in the capillaries of the tumors. However, our findings do not exclude the possibility that SDF-1/CXCR4 axis neutralization inhibits bone marrow–dependent tumor vasculogenesis, as is the case for embryonic vasculogenesis (42), because peripheral blood–derived late-outgrowth colonies expressed CXCR4 (Fig. 4*C*; ref. 43). The proportion of bone marrow–derived endothelial cells incorporated during neovascularization might differ among tumor types (44, 45) or might be influenced by the local expression profiles of various cytokines or growth factors (46). A recent study reported that *in vivo* expression of SDF-1 in ischemic tissues and CXCR4-positive progenitor recruitment were enhanced by the transcription factor hypoxia-inducible factor-1 (HIF-1; ref. 47). In another report, the metastatic ability of cancer cells was regulated by HIF-1-dependent CXCR4 expression (48). These findings suggest that HIF-1 expression in tumors might affect the recruitment of CXCR4-positive endothelial progenitors. Therefore, the degree of angiogenic inhibition by CXCR4 neutralization might increase in proportion to the contribution made by the recruitment of bone marrow–derived CXCR4-positive progenitors. Further experiments should be conducted in tumors of different origins to analyze the variation in the contribution of bone marrow–dependent vasculogenesis to tumor angiogenesis and the antitumor effects of the blockade of CXCR4.

Inhibitors of angiogenesis, such as anti-VEGF antibody, are expected to be able to suppress the advancement of tumor growth (49, 50). Treatment with bevacizumab, a monoclonal antibody against VEGF, in combination with fluorouracil/leucovorin treatment resulted in higher response rates and longer median survival times than treatment with fluorouracil/leucovorin alone (51). Moreover, because neovascularization processes are not continuously active in adult tissues, the targeting of vasculogenic reactions would be a relatively tumor-specific therapy (52). In contrast to the strategies employed by many anticancer drugs, strategies that target specific molecules might induce selective effects against cancer tissues. For example, the actions and interactions of endothelial cells and pericytes in tumors are qualitatively different from those in normal tissues (53), which might permit the specific targeting of the tumor vasculature. Indeed, SU6668, an inhibitor of VEGF and PDGF receptors, disrupted the association of pericytes with endothelium and reduced the vascularity in tumor tissues only (54).

Our experiments showed that injection of anti-CXCR4 antibody caused no critical bone marrow suppression or ischemic event.

Table 1. Peripheral blood cell counts in mice treated with normal IgG or anti-CXCR4 antibody

Treatment	Cancer cell type	RBC (×10,000/mm^3)	Hemoglobin (g/dL)	WBC (/μL)
Normal IgG	Colon38	878 ± 33	14.3 ± 0.52	3367 ± 376
Anti-CXCR4	Colon38	901 ± 28^{NS}	14.5 ± 0.35^{NS}	3200 ± 173^{NS}
Normal IgG	PancO2	802 ± 46	14.2 ± 0.18	2233 ± 376
Anti-CXCR4	PancO2	853 ± 38^{NS}	13.8 ± 0.45^{NS}	3133 ± 286^{NS}

NOTE: Peripheral blood cells were counted on day 14 after tumor inoculation (n = 3 for each group). NS, not significantly different versus normal IgG-treated mice.

Based on our data, the inhibition of vasculogenesis by CXCR4 neutralization might be cooperatively effective against tumors in combination with other angiogenic inhibitors, such as anti-VEGF antibody or chemotherapeutic drugs. In the future, combined strategies that include targeting SDF-1/CXCR4 might be promising anticancer therapies against a broad spectrum of cancers.

Acknowledgments

Received 10/25/2004; revised 3/16/2005; accepted 4/22/2005.

The costs of publication of this article were defrayed in part by the payment of page charges. This article must therefore be hereby marked *advertisement* in accordance with 18 U.S.C. Section 1734 solely to indicate this fact.

We thank Mitsuko Tsubouchi and members of the Sata Laboratory for their technical assistance.

References

1. Salvucci O, Yao L, Villalba S, Sajewicz A, Pittaluga S, Tosato G. Regulation of endothelial cell branching morphogenesis by endogenous chemokine stromal-derived factor-1. Blood 2002;99:2703–11.
2. Muller A, Homey B, Soto H, et al. Involvement of chemokine receptors in breast cancer metastasis. Nature 2001;410:50–6.
3. Federsppiel B, Melhado IG, Duncan AM, et al. Molecular cloning of the cDNA and chromosomal localization of the gene for a putative seven-transmembrane segment (7-TMS) receptor isolated from human spleen. Genomics 1993;16:707–12.
4. Baggiolini M. Chemokines and leukocyte traffic. Nature 1998;392:565–8.
5. Volin MV, Joseph L, Shockley MS, Davies PF. Chemokine receptor CXCR4 expression in endothelium. Biochem Biophys Res Commun 1998;242:46–53.
6. Feil C, Augustin HG. Endothelial cells differentially express functional CXC-chemokine receptor-4 (CXCR-4/fusin) under the control of autocrine activity and exogenous cytokines. Biochem Biophys Res Commun 1998;247:38–45.
7. Ganju RK, Brubaker SA, Meyer J, et al. The α-chemokine, stromal cell-derived factor-1α, binds to the transmembrane G-protein-coupled CXCR-4 receptor and activates multiple signal transduction pathways. J Biol Chem 1998;273:23169–75.
8. Ara T, Tokoyoda K, Sugiyama T, Egawa T, Kawabata K, Nagasawa T. Long-term hematopoietic stem cells require stromal cell-derived factor-1 for colonizing bone marrow during ontogeny. Immunity 2003;19:257–67.
9. Bachelder RE, Wendt MA, Mercurio AM. Vascular endothelial growth factor promotes breast carcinoma invasion in an autocrine manner by regulating the chemokine receptor CXCR4. Cancer Res 2002;62:7203–6.
10. Zeelenberg IS, Ruuls-Van Stalle L, Roos E. The chemokine receptor CXCR4 is required for outgrowth of colon carcinoma micrometastases. Cancer Res 2003;63:3833–9.
11. Kang Y, Siegel PM, Shu W, et al. A multigenic program mediating breast cancer metastasis to bone. Cancer Cell 2003;3:537–49.
12. Lee BC, Lee TH, Avraham S, Avraham HK. Involvement of the chemokine receptor CXCR4 and its ligand stromal cell-derived factor 1α in breast cancer cell migration through human brain microvascular endothelial cells. Mol Cancer Res 2004;2:327–38.
13. Libura J, Drukala J, Majka M, et al. CXCR4-SDF-1 signaling is active in rhabdomyosarcoma cells and regulates locomotion, chemotaxis, and adhesion. Blood 2002;100:2597–606.
14. Robledo MM, Bartolome RA, Longo N, et al. Expression of functional chemokine receptors CXCR3 and CXCR4 on human melanoma cells. J Biol Chem 2001;276:45098–105.
15. Murakami T, Maki W, Cardones AR, et al. Expression of CXC chemokine receptor-4 enhances the pulmonary metastatic potential of murine B16 melanoma cells. Cancer Res 2002;62:7328–34.
16. Asahara T, Masuda H, Takahashi T, et al. Bone marrow origin of endothelial progenitor cells responsible for postnatal vasculogenesis in physiological and pathological neovascularization. Circ Res 1999;85:221–8.
17. Lyden D, Hattori K, Dias S, et al. Impaired recruitment of bone-marrow-derived endothelial and hematopoietic precursor cells blocks tumor angiogenesis and growth. Nat Med 2001;7:1194–201.
18. Gill M, Dias S, Hattori K, et al. Vascular trauma induces rapid but transient mobilization of VEGFR2(+)AC133(+) endothelial precursor cells. Circ Res 2001;88:167–74.
19. McGrath KE, Koniski AD, Maltby KM, McGann JK, Palis J. Embryonic expression and function of the chemokine SDF-1 and its receptor, CXCR4. Dev Biol 1999;213:442–56.
20. Tachibana K, Hirota S, Iizasa H, et al. The chemokine receptor CXCR4 is essential for vascularization of the gastrointestinal tract. Nature 1998;393:591–4.
21. Takakura N, Watanabe T, Suenobu S, et al. A role for hematopoietic stem cells in promoting angiogenesis. Cell 2000;102:199–209.
22. Okabe M, Ikawa M, Kominami K, Nakanishi T, Nishimune Y. "Green mice" as a source of ubiquitous green cells. FEBS Lett 1997;407:313–9.
23. Tsuruo T, Yamori T, Tsukagoshi S, Sakurai Y. Enhanced cytocidal action of methotrexate by conjugation to concanavalin A. Int J Cancer 1980;26:655–9.
24. Morikane K, Tempero RM, Sivinski CL, et al. Organ-specific pancreatic tumor growth properties and tumor immunity. Cancer Immunol Immunother 1999;47:287–96.
25. Miyagishi M, Taira K. U6 promoter-driven siRNAs with four uridine 3′ overhangs efficiently suppress targeted gene expression in mammalian cells. Nat Biotechnol 2002;20:497–500.
26. Jazag A, Ijichi H, Kanai F, et al. Smad4 silencing in pancreatic cancer cell lines using stable RNA interference and gene expression profiles induced by transforming growth factor-β. Oncogene 2005;24:662–71.
27. Sata M, Saiura A, Kunisato A, et al. Hematopoietic stem cells differentiate into vascular cells that participate in the pathogenesis of atherosclerosis. Nat Med 2002;8:403–9.
28. Radoja S, Saio M, Schaer D, Koneru M, Vukmanovic S, Frey AB. CD8(+) tumor-infiltrating T cells are deficient in perforin-mediated cytolytic activity due to defective microtubule-organizing center mobilization and lytic granule exocytosis. J Immunol 2001;167:5042–51.
29. Wright DE, Bowman EP, Wagers AJ, Butcher EC, Weissman IL. Hematopoietic stem cells are uniquely selective in their migratory response to chemokines. J Exp Med 2002;195:1145–54.
30. Tanaka K, Sata M, Hirata Y, Nagai R. Diverse contribution of bone marrow cells to neointimal hyperplasia after mechanical vascular injuries. Circ Res 2003;93:783–90.
31. Tateishi K, Omata M, Tanaka K, Chiba T. The NEDD8 system is essential for cell cycle progression and morphogenetic pathway in mice. J Cell Biol 2001;155:571–9.
32. Petit I, Szyper-Kravitz M, Nagler A, et al. G-CSF induces stem cell mobilization by decreasing bone marrow SDF-1 and up-regulating CXCR4. Nat Immunol 2002;3:687–94.
33. Kanai F, Kawakami T, Hamada H, et al. Adenovirus-mediated transduction of *Escherichia coli* uracil phosphoribosyltransferase gene sensitizes cancer cells to low concentrations of 5-fluorouracil. Cancer Res 1998;58:1946–51.
34. Abbott JD, Huang Y, Liu D, Hickey R, Krause DS, Giordano FJ. Stromal cell-derived factor-1α plays a critical role in stem cell recruitment to the heart after myocardial infarction but is not sufficient to induce homing in the absence of injury. Circulation 2004;110:3300–5.
35. Crosby JR, Kaminski WE, Schatteman G, et al. Endothelial cells of hematopoietic origin make a significant contribution to adult blood vessel formation. Circ Res 2000;87:728–30.
36. Schlingemann RO, Rietveld FJ, de Waal RM, Ferrone S, Ruiter DJ. Expression of the high molecular weight melanoma-associated antigen by pericytes during angiogenesis in tumors and in healing wounds. Am J Pathol 1990;136:1393–405.
37. Asahara T, Murohara T, Sullivan A, et al. Isolation of putative progenitor endothelial cells for angiogenesis. Science 1997;275:964–7.
38. Coussens LM, Werb Z. Inflammation and cancer. Nature 2002;420:860–7.
39. Carmeliet P. Mechanisms of angiogenesis and arteriogenesis. Nat Med 2000;6:389–95.
40. Zou YR, Kottmann AH, Kuroda M, Taniuchi I, Littman DR. Function of the chemokine receptor CXCR4 in haematopoiesis and in cerebellar development. Nature 1998;393:595–9.
41. Smith MC, Luker KE, Garbow JR, et al. CXCR4 regulates growth of both primary and metastatic breast cancer. Cancer Res 2004;64:8604–12.
42. Carmeliet P. Angiogenesis in health and disease. Nat Med 2003;9:653–60.
43. Yamaguchi J, Kusano KF, Masuo O, et al. Stromal cell-derived factor-1 effects on *ex vivo* expanded endothelial progenitor cell recruitment for ischemic neovascularization. Circulation 2003;107:1322–8.
44. Ruzinova MB, Schoer RA, Gerald W, et al. Effect of angiogenesis inhibition by Id loss and the contribution of bone-marrow-derived endothelial cells in spontaneous murine tumors. Cancer Cell 2003;4:277–89.
45. Sikder H, Huso DL, Zhang H, et al. Disruption of Id1 reveals major differences in angiogenesis between transplanted and autochthonous tumors. Cancer Cell 2003;4:291–9.
46. Takahashi T, Kalka C, Masuda H, et al. Ischemia- and cytokine-induced mobilization of bone marrow-derived endothelial progenitor cells for neovascularization. Nat Med 1999;5:434–8.
47. Ceradini DJ, Kulkarni AR, Callaghan MJ, et al. Progenitor cell trafficking is regulated by hypoxic gradients through HIF-1 induction of SDF-1. Nat Med 2004;10:858–64.
48. Staller P, Sulitkova J, Lisztwan J, Moch H, Oakeley EJ, Krek W. Chemokine receptor CXCR4 downregulated by von Hippel-Lindau tumour suppressor pVHL. Nature 2003;425:307–11.
49. Kerbel R, Folkman J. Clinical translation of angiogenesis inhibitors. Nat Rev Cancer 2002;2:727–39.
50. Willett CG, Boucher Y, di Tomaso E, et al. Direct evidence that the VEGF-specific antibody bevacizumab has antivascular effects in human rectal cancer. Nat Med 2004;10:145–7.
51. Kabbinavar F, Hurwitz HI, Fehrenbacher L, et al. Phase II, randomized trial comparing bevacizumab plus fluorouracil (FU)/leucovorin (LV) with FU/LV alone in patients with metastatic colorectal cancer. J Clin Oncol 2003;21:60–5.
52. Carmeliet P, Moons L, Luttun A, et al. Synergism between vascular endothelial growth factor and placental growth factor contributes to angiogenesis and plasma extravasation in pathological conditions. Nat Med 2001;7:575–83.
53. Jain RK. Determinants of tumor blood flow: a review. Cancer Res 1988;48:2641–58.
54. Bergers G, Song S, Meyer-Morse N, Bergsland E, Hanahan D. Benefits of targeting both pericytes and endothelial cells in the tumor vasculature with kinase inhibitors. J Clin Invest 2003;111:1287–95.

Chemosensitivity profile of cancer cell lines and identification of genes determining chemosensitivity by an integrated bioinformatical approach using cDNA arrays

Noriyuki Nakatsu,[1,2] Yoko Yoshida,[1] Kanami Yamazaki,[1] Tomoki Nakamura,[1] Shingo Dan,[1] Yasuhisa Fukui,[3] and Takao Yamori[1]

[1]Division of Molecular Pharmacology, Cancer Chemotherapy Center, Japanese Foundation for Cancer Research; [2]Division of Cellular and Molecular Toxicology, Biological Safety Research Center, National Institute of Health Sciences; and [3]Laboratory of Biological Chemistry, Department of Applied Biological Chemistry, Faculty of Agricultural and Life Science, University of Tokyo, Tokyo, Japan

Abstract

We have established a panel of 45 human cancer cell lines (JFCR-45) to explore genes that determine the chemosensitivity of these cell lines to anticancer drugs. JFCR-45 comprises cancer cell lines derived from tumors of three different organs: breast, liver, and stomach. The inclusion of cell lines derived from gastric and hepatic cancers is a major point of novelty of this study. We determined the concentration of 53 anticancer drugs that could induce 50% growth inhibition (GI_{50}) in each cell line. Cluster analysis using the GI_{50}s indicated that JFCR-45 could allow classification of the drugs based on their modes of action, which coincides with previous findings in NCI-60 and JFCR-39. We next investigated gene expression in JFCR-45 and developed an integrated database of chemosensitivity and gene expression in this panel of cell lines. We applied a correlation analysis between gene expression profiles and chemosensitivity profiles, which revealed many candidate genes related to the sensitivity of cancer cells to anticancer drugs. To identify genes that directly determine chemosensitivity, we further tested the ability of these candidate genes to alter sensitivity to anticancer drugs after individually overexpressing each gene in human fibrosarcoma HT1080. We observed that transfection of HT1080 cells with the *HSPA1A* and *JUN* genes actually enhanced the sensitivity to mitomycin C, suggesting the direct participation of these genes in mitomycin C sensitivity. These results suggest that an integrated bioinformatical approach using chemosensitivity and gene expression profiling is useful for the identification of genes determining chemosensitivity of cancer cells. [Mol Cancer Ther 2005;4(3):399–412]

Introduction

Predicting the chemosensitivity of individual patients is important to improve the efficacy of cancer chemotherapy. An approach to this end is to understand the genes that determine the chemosensitivity of cancer cells. Many genes have been described that determine the sensitivity to multiple drugs, including drug transporters (1-3) and metabolizing enzymes (4-6). Genes determining the sensitivity to specific drugs have also been reported. For example, increased activities of γ-glutamyl hydrolase (7) and dihydrofolate reductase (8) are resistant factors for methotrexate; increased activities of thymidylate synthase (9), metallothionein (10), and cytidine deaminase (11) are resistant factors for 5-fluorouracil (5-FU), cisplatin, 1-β-D-arabinofuranosylcytosine, respectively; and increased activity of NQO1 (12) is a sensitive factor for mitomycin C (MMC). However, the chemosensitivity of cancer cells is not determined by a handful of genes. These genes are not sufficient to explain the variation of the chemosensitivity of cancer cells.

Recently, attempts were made to predict the chemosensitivity of cancers using genome-wide expression profile analyses, such as cDNA microarray and single nucleotide polymorphisms (13–18). For example, Scherf et al. (18) and Zembutsu et al. (15) reported the analysis of genes associated with sensitivity to anticancer drugs in a panel of human cancer cell lines and in human cancer xenografts, respectively. Tanaka et al. (17) presented prediction models of anticancer efficacy of eight drugs using real-time PCR expression analysis of 12 genes in cancer cell lines and clinical samples. We also analyzed chemosensitivity-related genes in 39 human cancer cell lines (JFCR-39; ref. 19) and validated the association of some of these genes to chemosensitivity using additional cancer cell lines (20). These genes can be used as markers to predict chemosensitivity. Moreover, some of these genes may directly determine the chemosensitivity of cancer cells.

In the present study, we established a new panel of 45 human cancer cell lines (JFCR-45) derived from tumors from three different organs: breast, liver, and stomach. Using JFCR-45, we attempted to analyze the heterogeneity of chemosensitivity in breast, liver, and stomach cancers. We assessed their sensitivity to 53 anticancer drugs and

Received 9/7/04; revised 12/16/04; accepted 1/25/05.

Grant support: Ministry of Education, Culture, Sports, Science and Technology of Japan Aid for Scientific Research on Priority Areas; Japan Society for the Promotion of Science Grants-in-Aid for Scientific Research (B) and Exploratory Research; and research grant from the Princess Takamatsu Cancer Research Fund.

The costs of publication of this article were defrayed in part by the payment of page charges. This article must therefore be hereby marked advertisement in accordance with 18 U.S.C. Section 1734 solely to indicate this fact.

Requests for reprints: Takao Yamori, Division of Molecular Pharmacology, Cancer Chemotherapy Center, Japanese Foundation for Cancer Research, 3-10-6, Ariake, Koto-ku, Tokyo 135-8550, Japan. Phone: 81-3-3520-0111; Fax: 81-3-3570-0484. E-mail: yamori@ims.u-tokyo.ac.jp

developed a database of chemosensitivity. Then, we analyzed gene expression in 42 human cancer cell lines using cDNA arrays and stored them in the gene expression database. Using these two databases, we extracted genes whose expression was correlated to chemosensitivity. We further screened them to identify genes that could change the sensitivity to anticancer drugs using an *in vitro* gene transfection assay.

Materials and Methods

Cell Lines and Cell Cultures

We established a panel of JFCR-45 that included a portion of JFCR-39 and the 12 stomach cancer cell lines described previously (19, 20). They consist of the following cell lines: breast cancer cells HBC-4, BSY1, HBC-5, MCF-7, MDA-MB-231, KPL-3C (21), KPL-4, KPL-1, T-47D (22), HBC-9, ZR-75-1 (23), and HBC-8; liver cancer cells HepG2, Hep3B, Li-7, PLC/PRF/5, HuH7, HLE, HLF (24), HuH6 (25), RBE, SSP-25 (26), HuL-1 (27), and JHH-1 (28); and stomach cancer cells St-4, MKN1, MKN7, MKN28, MKN45, MKN74, GCIY, GT3TKB, HGC27, AZ521 (29), 4-1ST, NUGC-3, NUGC-3/5-FU, HSC-42, AGS, KWS-1, TGS-11, OKIBA, ISt-1, ALF, and AOTO. The AZ521 cell line was obtained from the Cell Resource Center for Biomedical Research, Institute of Development, Aging and Cancer, Tohoku University (Sendai, Japan). The 4-1ST, OKIBA, and AOTO cell lines were provided by Dr. Tokuji Kawaguchi (Department of Pathology, Cancer Institute, Japanese Foundation for Cancer Research, Tokyo, Japan). All cell lines were cultured in RPMI 1640 (Nissui Pharmaceutical, Tokyo, Japan) with 5% fetal bovine serum, penicillin (100 units/mL), and streptomycin (100 μg/mL) at 37°C under 5% CO_2.

Determination of the Sensitivity to Anticancer Drugs

Growth inhibition experiments were done to assess the chemosensitivity to anticancer drugs. Growth inhibition was measured by determining the changes in the amounts of total cellular protein after 48 hours of drug treatment using a sulforhodamine B assay. The GI_{50} values, which represent 50% growth inhibition concentration, were evaluated as described before (30, 31). Several experiments were done to determine the median GI_{50} value for each drug. Absolute values were then log transformed for further analysis.

Anticancer Drugs and Compounds

Actinomycin D, 5-FU, tamoxifen, cytarabine, radicicol, melphalan, 6-mercaptopurine, 6-thioguanine, and colchicine were purchased from Sigma (St. Louis, MO). The anticancer agents in clinical use were obtained from the company specified in parentheses, and those under development were kindly provided by the company specified as described below: aclarubicin and neocarzinostatin (Yamanouchi Pharmaceutical, Tokyo, Japan); oxaliplatin (Asahi Kasei, Tokyo, Japan), HCFU (Nihon Schering, Osaka, Japan); doxifluridine (Chugai Pharmaceutical, Tokyo, Japan); toremifene, bleomycin, and estramustine (Nippon Kayaku, Tokyo, Japan); daunorubicin and pirarubicin (Meiji, Tokyo, Japan); doxorubicin, epirubicin, MMC, vinorelbine, and L-asparaginase (Kyowa Hakko Kogyo, Tokyo, Japan); peplomycin, etoposide, NK109, and NK611 (Nippon Kayaku); vinblastine, vincrinstine, IFN-γ, and 4-hydroperoxycyclophosphamide (Shionogi, Tokyo, Japan); carboplatin and cisplatin (Bristol-Myers Squibb, New York, NY); mitoxantrone and methotrexate (Wyeth Lederie Japan, Tokyo, Japan); cladribine (Janssen Pharmaceutical, Titusville, NJ); amsacrine (Pfizer Pharmaceutical, formerly Warner Lambert, Plymouth, MI); camptothecin, irinotecan, and SN-38 (Yakult, Tokyo, Japan); paclitaxel (Bristol-Myers Squibb); docetaxel and topotecan (Aventis Pharma, Strasbourg, France); IFN-α (Sumitomo Pharmaceutical, Osaka, Japan); IFN-β (Daiichi Pharmaceutics, Tokyo, Japan); gemcitabine (Eli Lilly Japan, Kobe, Japan); E7010 and E7070 (Eisai, Tokyo, Japan); dolastatine 10 (Teikoku Hormone MFG, Tokyo, Japan); and TAS103 (Taiho Pharmaceutical Co., Tokyo, Japan).

Gene Expression Profiles by cDNA Array

Expression profiles of 3,537 genes in 42 human cancer cell lines were examined using Atlas Human 3.6 Array (BD Biosciences Clontech, Inc., Franklin Lakes, NJ) in duplicates. Experiments were done according to the manufacturer's instructions. Briefly, cell lines were harvested in log phase. Total RNA was extracted with TRIzol reagent (Invitrogen, Inc., Carlsbad, CA) and purified with Atlas Pure Total RNA Labeling System. Purified total RNAs were converted to ^{32}P-labeled cDNA probe by SuperScript II (Invitrogen). cDNA probe was hybridized to the Atlas Array overnight at 68°C and washed. Hybridized array was detected with PhosphorImager (Molecular Dynamics, Inc., Sunnyvale, CA). Scanned data were transformed to the numerical value with Atlas Image 2.0 software (BD Biosciences Clontech) and normalized by dividing by the value of 90% percentile of all genes in each experiment. Then, the intensities of the genes were defined by the average of intensities of duplicate results. The genes whose expression levels differed more than twice between the duplicates were eliminated from subsequent analysis. When the intensities of gene expression in both arrays were below the threshold value, they were given the value of threshold and were used for analysis. We determined the values of threshold of the normalized data as 30% of the value of 90% percentile. Then, $\log_2$ was calculated for each expression value.

Hierarchical Clustering

Hierarchical clustering using average linkage method was done by "Gene Spring" software (Silicon Genetics, Inc., Redwood, CA). Pearson correlation coefficients were used to determine the degree of similarity.

Correlation Analysis between Gene Expression and Chemosensitivity Profiles

The genes whose expressions were observed in >50% of all cell lines examined were selected for the correlation analysis. The degree of similarity between chemosensitivity and gene expression were calculated using the following Pearson correlation coefficient formula:

$$r = \frac{\sum_i (x_i - x_m)(y_i - y_m)}{\sqrt{\sum_i (x_i - x_m)^2 \sum_i (y_i - y_m)^2}}$$

where x_i is the log expression data of the gene x in cell i, y_i is the log sensitivity $|\log_{10}GI_{50}|$ of cell i to drug y, x_m is the mean of the log expression data of the gene x, and y_m is the mean sensitivity $|\log_{10}GI_{50}|$ of drug y. A significant correlation was defined as $P < 0.05$.

Screening of the Genes That Determine Chemosensitivity

Candidate genes related to the chemosensitivity were cloned into the vector pcDNA3.1/*myc*-His A (Invitrogen). Transfection of HT1080 cells with the plasmid DNA was carried out using LipofectAMINE Plus reagent (Invitrogen). The transfection efficiency was monitored by green fluorescent protein fluorescence. The fluorescence of green fluorescent protein was observed in >90% of the green fluorescent protein–transfected HT1080 (data not shown). Twenty-four hours after the transfection, proper concentrations of MMC were added and the cells were treated for 24 hours. Efficacies of anticancer drugs were determined by measuring the growth inhibition. Cell growth was measured by following [^{3}H]thymidine incorporation. [^{3}H]thymidine (0.067 MBq) was added to each well and incubated at 37°C for 45 minutes. Cells were washed with prewarmed PBS(−) and fixed with 10% TCA on ice for 2 hours. After fixing, cells were washed with 10% TCA and lysed with 0.1% SDS-0.2 N NaOH solution. After incubation at 37°C, the lysed mixture was neutralized with 0.25 mol/L acetic acid solution. [^{3}H]thymidine incorporated into the cells was determined using scintillation counter. All experiments, except for interleukin (IL)-18, were done four times.

Results

Sensitivity of JFCR-45 to 53 Anticancer Drugs

Sensitivity to 53 drugs was assessed as described in Materials and Methods. The known modes of actions and the value of $|\log_{10}GI_{50}|$ of 53 anticancer drugs in each of the 45 cell lines are summarized in Table 1. The $|\log_{10}GI_{50}|$ indicated here is the median value of multiple experiments. The chemosensitivity of the cell lines differed even among those derived from the same organ. These data were stored in a chemosensitivity database. Figure 1 shows the classification of the anticancer drugs by hierarchical clustering analysis based on chemosensitivity, $|\log_{10}GI_{50}|$, of JFCR-45. As shown, the 53 drugs were classified into several clusters, each consisting of drugs with similar modes of action [e.g., one cluster included topoisomerase (topo) I inhibitors, such as camptothecin, topotecan, and SN-38]. The second cluster comprised tubulin binders, including taxanes and *Vinca* alkaloids. 5-FU and its derivatives were also clustered into a single group. These results indicated that our system using JFCR-45 was able to classify the drugs based on their modes of action, which is in agreement with previous findings using NCI-60 and JFCR-39 (18, 19, 32).

Classification of 42 Human Cancer Cell Lines According to Gene Expression Profiles

Using a cDNA array, we examined the expression of 3,537 genes in 42 cell lines of JFCR-45. Based on these expression profiles, hierarchical clustering was done. In a few experiments, cell lines derived from the same organ were clustered into a group (Fig. 2). Breast cancer cell lines, except KPL-4, formed one cluster. Liver and stomach

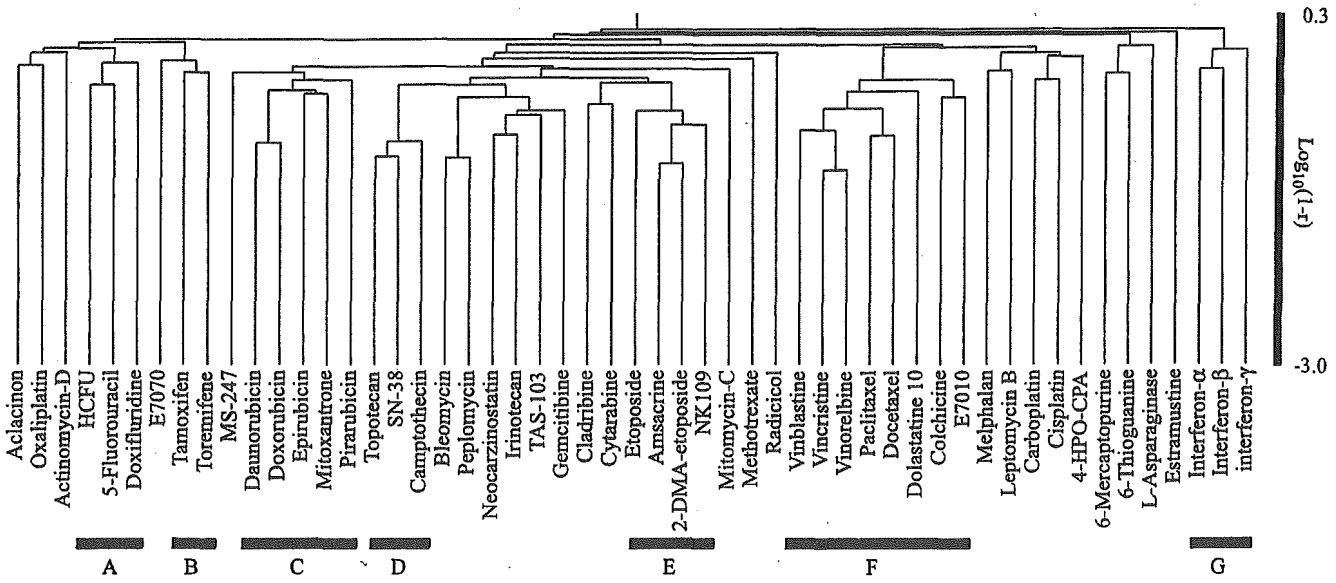

Figure 1. Hierarchical clustering of 53 anticancer drugs based on their activity on 45 human cancer cell lines. Hierarchical clustering method was "average linkage method" using Pearson correlation as distance. Fifty-three drugs were classified into several clusters, each consisting of drugs with similar modes of action or targets: (**A**) 5-FU derivatives, (**B**) estrogen receptor, (**C**) DNA synthesis/topo II inhibitors, (**D**) topo I inhibitors, (**E**) topo II inhibitors, (**F**) tubulin binders, and (**G**) IFN.

Table 1. The mode of actions and the median value of $|\log_{10}GI_{50}|$ of 53 anticancer drugs in each of the 45 cell lines

Drug name	Target/ mode of action	Breast											
		HBC-4	BSY1	HBC-5	MCF-7	MDA-MB-231	KPL-3C	KPL-4	KPL-1	T-47D	HBC-9	ZR-75-1	HBC-8
Aclarubicin	DNA/RNA synthesis	7.04	8.69	7.92	7.86	7.83	7.11	7.63	7.95	7.39	7.08	8.03	7.93
Oxaliplatin	DNA cross-linker	5.79	5.75	5.40	5.69	4.75	5.04	5.20	4.78	5.17	4.10	5.08	6.17
Actinomycin D	RNA synthesis	9.20	9.10	8.85	9.45	8.71	8.90	9.05	9.04	8.89	8.24	8.98	9.60
HCFU	Pyrimidine	4.36	5.17	4.44	5.13	4.57	4.65	5.55	4.41	4.97	4.22	4.68	4.84
5-FU	Pyrimidine	4.43	4.87	4.40	5.12	4.18	4.00	5.23	4.00	4.13	4.00	4.70	5.11
Doxifluridine	Pyrimidine	4.00	4.42	4.00	4.00	4.00	4.00	4.09	4.00	4.00	4.00	4.14	4.19
E7070	Cell cycle inhibitor	4.50	6.20	4.22	4.50	4.35	4.94	5.01	4.74	4.69	4.00	4.38	4.98
Tamoxifen	Estrogen receptor	4.95	5.42	5.01	5.04	4.90	5.14	5.49	4.93	5.31	4.90	4.95	5.53
Toremifene	Estrogen receptor	4.81	5.12	4.87	4.96	4.85	4.93	5.13	4.88	5.17	4.89	4.88	4.86
MS-247	DNA synthesis	6.08	6.79	5.32	6.78	5.98	6.09	6.16	5.86	6.63	6.42	6.88	6.71
Daunorubicin	DNA synthesis/topo II	6.96	7.34	6.82	7.68	6.83	6.77	7.25	6.84	7.41	6.92	7.39	7.97
Doxorubicin	DNA synthesis/topo II	7.13	7.26	6.85	7.58	6.66	6.74	7.38	6.76	7.36	6.94	7.12	7.85
Epirubicin	DNA synthesis/topo II	6.08	6.90	6.59	7.08	6.42	6.50	7.03	6.83	7.26	6.73	7.90	7.19
Mitoxantrone	DNA synthesis	6.28	7.12	6.00	8.06	6.50	6.40	6.83	6.38	7.11	6.96	8.02	7.44
Pirarubicin	DNA synthesis/topo II	8.97	9.00	8.34	9.00	8.47	8.62	9.00	8.39	9.00	8.22	9.00	9.00
Topotecan	Topo I	5.84	6.57	5.10	8.00	5.55	6.37	6.71	5.90	7.51	6.18	7.20	7.61
SN-38	Topo I	7.98	7.52	5.56	8.56	6.12	6.75	7.40	6.60	8.25	6.13	7.92	7.75
Camptothecin	Topo I	5.92	6.57	6.04	7.63	5.86	6.67	6.60	6.70	7.12	5.80	7.21	6.92
Bleomycin	DNA synthesis	4.81	4.89	4.00	4.48	4.00	4.00	5.59	4.00	5.46	4.46	4.22	4.37
Peplomycin	DNA synthesis	4.90	5.84	4.00	5.22	4.27	4.61	6.29	4.08	5.37	4.52	4.72	5.25
Neocarzinostatin	DNA synthesis	7.35	8.00	6.03	8.17	6.55	6.42	7.61	6.18	7.26	7.06	7.26	8.10
Irinotecan	Topo I	4.86	5.09	4.00	5.46	4.28	4.30	4.91	4.11	5.21	4.15	4.47	5.24
TAS103	Topo	6.81	7.22	6.37	7.66	6.57	6.45	7.20	6.17	7.25	6.16	7.13	7.60
Gemcitabine	Pyrimidine	6.74	5.62	4.00	8.00	5.20	4.00	7.25	4.00	7.18	5.15	4.71	5.75
Cladribine	Pyrimidine	4.00	4.00	4.00	5.41	4.05	4.60	4.73	4.00	4.83	4.23	4.00	4.68
Cytarabine	Pyrimidine	4.00	4.00	4.00	6.40	4.00	4.00	5.02	4.00	4.00	4.00	4.00	4.54
Etoposide	Topo II	4.88	5.48	4.39	6.15	4.66	4.00	5.42	4.68	5.93	4.48	5.11	4.72
Amsacrine	Topo II	5.20	5.78	5.29	6.56	5.25	4.89	5.69	4.93	5.97	5.14	6.56	5.70
2-Dimethylaminoetoposide	Topo II	4.67	4.82	4.02	6.02	4.48	4.00	5.03	4.00	5.05	4.89	5.74	4.71
NK109	Topo II	5.69	5.88	5.27	6.37	6.04	5.49	6.31	5.56	6.30	5.57	6.08	5.81
MMC	DNA alkylator	5.90	6.68	5.68	6.99	5.14	5.46	6.40	5.50	5.42	5.49	5.74	6.69
Methotrexate	DHFR	7.11	5.19	4.00	7.53	4.00	4.00	7.53	5.25	4.00	4.00	4.00	4.00
Radicicol	HSP90/Tyr kinase	5.55	5.80	5.17	7.28	6.55	5.19	6.13	5.28	7.43	5.39	6.18	6.62
Vinblastine	Tubulin	9.22	9.76	9.22	9.68	8.67	9.17	9.77	9.13	9.15	6.00	7.58	7.99
Vincristine	Tubulin	8.77	9.72	9.29	9.42	8.67	9.12	9.57	9.31	9.22	6.00	8.41	6.20
Vinorelbine	Tubulin	8.45	9.23	8.51	8.85	8.23	8.33	9.35	8.93	8.41	6.00	8.16	6.00
Paclitaxel	Tubulin	7.30	8.43	7.94	7.72	7.37	7.38	8.20	7.53	7.90	6.00	7.05	6.59
Docetaxel	Tubulin	8.41	8.98	8.23	8.52	7.88	8.18	8.82	8.19	8.56	6.00	7.15	8.28
Dolastatine 10	Tubulin	9.15	10.83	11.19	10.26	9.07	10.02	10.74	9.44	9.95	8.00	9.46	8.67
Colchicine	Tubulin	6.06	8.68	6.33	6.48	7.24	7.58	8.48	7.89	6.64	5.00	7.84	6.59
E7010	Tubulin	4.37	6.56	4.00	6.14	5.07	5.38	6.69	5.71	6.29	5.50	6.04	4.72
Melphalan	DNA cross-linker	4.20	4.92	4.42	5.09	4.33	4.67	4.04	4.66	4.38	4.08	4.45	4.57
Leptomycin B	Cell cycle inhibitor	9.35	9.64	9.33	9.44	8.91	9.59	9.47	9.63	9.26	8.96	9.78	9.74
Carboplatin	DNA cross-linker	4.00	4.34	4.12	4.00	4.00	4.00	4.00	4.00	4.00	4.00	4.00	4.00
Cisplatin	DNA cross-linker	4.90	5.69	5.65	5.09	4.56	4.72	5.52	4.63	4.56	5.35	4.71	5.39
4-Hydroperoxycyclo-phosphamide	DNA alkylator	4.78	4.85	5.41	5.58	4.68	4.78	4.54	4.74	4.86	5.18	4.76	4.78
6-Mercaptopurine	Purine	5.41	4.73	4.15	5.88	5.17	5.11	4.50	5.02	6.00	4.27	4.05	4.50
6-Thioguanine	Purine	4.59	5.85	5.40	5.86	5.80	5.92	5.55	5.91	5.81	4.53	5.21	5.66
L-Asparaginase	Protein synthesis	6.55	6.63	4.00	6.43	6.01	6.03	7.20	6.18	6.10	5.49	6.07	6.36
Estramustine	Estradiol	4.09	4.51	4.00	4.00	4.66	4.85	4.56	4.31	4.17	4.74	4.00	4.73
IFN-α	Biological response	4.00	7.71	4.00	4.00	4.23	4.00	4.00	4.00	4.00	4.00	4.00	5.02
IFN-β	Biological response	4.00	8.00	4.00	4.00	6.40	4.23	7.08	4.00	4.00	4.00	4.00	4.56
IFN-γ	Biological response	7.69	7.93	4.00	4.00	4.00	4.00	4.00	4.00	4.00	4.00	4.00	4.00

(Continued on the following page)

Table 1. The mode of actions and the median value of $|\log_{10}GI_{50}|$ of 53 anticancer drugs in each of the 45 cell lines (Cont'd)

Drug name	Target/ mode of action	Liver											
		HepG2	Hep3B	Li-7	PLC/ PRF/5	HuH7	HLE	HLF	HuH6	RBE	SSP-25	HuL-1	JHH-1
Aclarubicin	DNA/RNA synthesis	8.13	7.77	7.39	7.68	8.29	7.49	7.86	7.70	7.87	7.39	7.97	8.23
Oxaliplatin	DNA cross-linker	7.07	5.39	5.78	5.61	6.44	4.90	4.75	5.60	5.19	4.58	6.04	6.01
Actinomycin D	RNA synthesis	9.03	8.61	8.24	8.04	8.99	8.13	8.45	8.75	8.25	8.47	8.78	9.00
HCFU	Pyrimidine	5.28	4.80	4.79	4.56	4.99	4.67	4.70	4.50	4.92	4.69	4.87	4.63
5-FU	Pyrimidine	5.27	4.20	4.26	4.21	5.08	4.00	4.19	4.00	4.60	4.00	5.29	4.72
Doxifluridine	Pyrimidine	4.49	4.00	4.00	4.00	4.00	4.00	4.00	4.00	4.00	4.00	4.04	4.00
E7070	Cell cycle inhibitor	5.47	4.99	4.77	4.44	5.36	4.61	4.43	4.74	5.09	4.29	4.29	4.87
Tamoxifen	Estrogen receptor	5.45	5.30	5.23	4.79	5.09	5.02	4.97	5.38	4.90	5.11	4.87	4.97
Toremifene	Estrogen receptor	5.06	4.97	4.92	4.82	4.99	5.09	4.91	4.95	4.92	5.00	4.80	5.10
MS-247	DNA synthesis	6.33	5.84	6.35	5.23	6.02	6.58	6.42	5.82	5.66	6.37	5.67	6.82
Daunorubicin	DNA synthesis/topo II	7.48	7.10	6.83	6.39	7.29	7.55	7.49	6.98	7.18	6.73	7.08	7.51
Doxorubicin	DNA synthesis/topo II	7.29	6.77	6.88	5.83	7.04	7.39	7.25	6.87	6.89	6.68	6.89	7.31
Epirubicin	DNA synthesis/topo II	7.33	6.86	6.87	6.29	7.31	7.21	7.25	6.91	6.84	6.73	6.74	7.03
Mitoxantrone	DNA synthesis	7.95	6.51	7.88	6.51	6.76	7.60	7.67	6.71	7.37	7.59	6.11	7.15
Pirarubicin	DNA synthesis/topo II	9.00	8.58	9.00	8.26	9.00	9.00	9.00	8.59	8.98	9.00	8.95	9.00
Topotecan	Topo I	7.93	5.81	7.70	5.64	6.07	7.73	7.73	5.72	6.83	6.74	5.30	6.99
SN-38	Topo I	8.43	6.37	8.21	6.03	6.75	8.28	8.31	5.91	7.05	7.47	5.69	7.74
Camptothecin	Topo I	7.44	6.19	7.48	5.86	6.35	7.42	7.53	6.10	6.69	6.79	6.16	6.92
Bleomycin	DNA synthesis	6.02	4.38	5.66	4.00	4.85	6.04	6.59	4.15	4.73	4.97	5.10	4.94
Peplomycin	DNA synthesis	6.73	4.72	6.40	4.45	5.46	5.86	6.56	4.01	5.12	5.83	5.35	5.34
Neocarzinostatin	DNA synthesis	8.22	6.72	7.81	6.34	6.92	7.60	7.80	6.57	7.27	7.53	6.67	7.09
Irinotecan	Topo I	5.18	4.36	5.61	4.00	4.33	5.25	5.13	4.11	4.37	4.64	4.05	4.78
TAS103	Topo	7.56	6.57	7.68	6.64	6.95	7.81	7.87	6.55	7.32	6.89	6.95	6.94
Gemcitabine	Pyrimidine	8.00	4.63	8.00	4.00	6.16	7.83	8.00	4.19	6.56	7.24	5.60	5.85
Cladribine	Pyrimidine	6.30	4.00	4.86	4.00	4.00	5.85	5.45	4.00	4.86	5.30	4.00	4.00
Cytarabine	Pyrimidine	6.22	4.00	4.00	4.00	4.00	5.22	5.41	4.00	4.00	4.00	4.00	4.00
Etoposide	Topo II	5.62	4.86	5.56	4.60	4.92	5.80	5.70	5.05	4.85	5.35	5.35	5.09
Amsacrine	Topo II	6.41	5.56	6.66	5.47	5.77	6.58	6.61	5.43	5.90	5.98	5.71	5.46
2-Dimethylaminoetoposide	Topo II	5.56	4.66	5.70	4.54	4.73	5.75	5.84	4.57	5.20	5.54	4.75	4.66
NK109	Topo II	6.56	5.96	6.72	5.85	6.05	6.83	6.77	5.84	6.24	6.39	5.92	6.09
MMC	DNA alkylator	6.56	5.04	7.09	5.63	5.73	6.15	6.31	5.38	5.32	6.20	5.50	5.99
Methotrexate	DHFR	7.47	4.00	6.11	4.00	6.12	6.64	6.83	4.00	6.71	4.06	4.00	5.13
Radicicol	HSP90/Tyr kinase	7.87	7.08	6.43	6.16	6.46	6.63	6.83	6.03	5.52	5.61	5.94	5.68
Vinblastine	Tubulin	8.18	6.50	9.30	7.73	9.35	9.73	9.20	7.22	6.00	9.51	9.11	9.66
Vincristine	Tubulin	7.93	6.00	7.70	6.00	8.52	8.76	8.40	6.00	6.00	8.27	8.38	9.11
Vinorelbine	Tubulin	7.98	6.00	8.15	6.00	8.43	8.75	8.28	7.05	6.00	8.51	8.65	9.21
Paclitaxel	Tubulin	7.35	6.84	7.41	6.48	7.44	7.50	7.27	6.00	6.73	7.80	8.22	7.94
Docetaxel	Tubulin	8.08	7.11	7.83	6.80	8.23	8.09	8.08	6.00	6.14	8.50	8.54	8.50
Dolastatine 10	Tubulin	10.42	8.94	10.71	9.50	10.12	10.19	9.94	8.60	8.00	10.30	9.68	10.61
Colchicine	Tubulin	7.16	5.40	7.25	6.43	7.62	7.77	7.39	5.54	5.00	7.50	7.45	8.17
E7010	Tubulin	6.28	4.62	6.38	6.23	6.35	6.47	6.35	4.79	4.00	6.50	6.44	6.50
Melphalan	DNA cross-linker	4.76	4.47	4.62	4.00	4.44	4.59	4.81	4.03	4.39	4.40	4.84	4.86
Leptomycin B	Cell cycle inhibitor	9.67	9.32	9.44	9.19	9.10	9.31	9.37	9.00	9.29	9.51	9.54	9.66
Carboplatin	DNA cross-linker	4.18	4.00	4.00	4.00	4.00	4.00	4.00	4.00	4.00	4.00	4.00	4.53
Cisplatin	DNA cross-linker	5.53	5.32	5.51	4.75	5.63	5.36	5.45	5.26	4.73	4.94	5.41	5.86
4-Hydroperoxycyclo-phosphamide	DNA alkylator	4.92	4.74	4.88	4.65	4.84	4.87	5.04	4.82	4.69	4.90	4.76	5.30
6-Mercaptopurine	Purine	5.01	4.10	5.12	4.42	4.00	4.17	4.49	4.90	5.29	4.58	4.82	5.10
6-Thioguanine	Purine	5.08	4.57	5.23	5.37	4.70	4.22	5.14	6.04	5.76	5.18	5.92	6.14
L-Asparaginase	Protein synthesis	6.40	4.78	8.00	6.49	4.00	6.91	6.63	4.00	6.35	8.00	6.61	4.42
Estramustine	Estradiol	4.00	4.00	4.27	4.24	4.05	4.37	4.03	4.10	4.14	4.18	4.09	4.14
IFN-α	Biological response	4.00	4.00	4.20	4.00	4.00	4.00	4.00	4.00	4.00	4.00	4.00	4.00
IFN-β	Biological response	4.00	4.00	7.15	6.17	4.00	4.00	4.00	4.00	4.00	4.00	4.00	4.00
IFN-γ	Biological response	4.00	4.00	4.00	4.00	4.00	4.00	4.00	4.00	4.00	4.00	4.00	7.93

(Continued on the following page)

Table 1. The mode of actions and the median value of $|\log_{10}GI_{50}|$ of 53 anticancer drugs in each of the 45 cell lines (Cont'd)

Drug name	Target/ mode of action	Stomach											
		St-4	MKN1	MKN7	MKN28	MKN45	MKN74	GCIY	GT3 TKB	HGC27	AZ521	4-1ST	NUGC -3
Aclarubicin	DNA/RNA synthesis	7.88	8.09	7.73	7.25	8.59	7.43	8.00	7.86	7.13	8.49	7.96	9.04
Oxaliplatin	DNA cross-linker	4.75	5.04	4.42	4.58	6.84	4.93	5.71	5.31	5.10	6.16	5.17	6.18
Actinomycin D	RNA synthesis	7.99	8.74	8.77	9.02	9.39	9.20	8.24	9.12	8.76	9.55	8.80	8.85
HCFU	Pyrimidine	4.17	4.70	4.82	4.77	5.56	4.86	4.77	5.09	4.74	5.21	4.84	4.74
5-FU	Pyrimidine	4.35	4.40	4.26	4.27	5.46	4.22	4.60	5.09	4.34	5.12	4.04	4.67
Doxifluridine	Pyrimidine	4.00	4.00	4.01	4.00	4.20	4.00	4.00	4.00	4.00	4.00	4.00	4.02
E7070	Cell cycle inhibitor	4.43	6.03	4.90	5.48	4.55	5.20	5.04	4.82	5.69	6.02	4.88	5.75
Tamoxifen	Estrogen receptor	4.95	4.89	5.44	5.23	5.13	5.67	4.92	5.19	5.25	5.11	4.87	5.06
Toremifene	Estrogen receptor	4.81	4.92	4.90	4.82	4.93	5.23	4.85	4.92	5.07	5.09	4.87	4.96
MS-247	DNA synthesis	5.66	5.72	6.27	5.59	7.32	6.62	5.71	6.88	6.76	7.58	7.09	6.62
Daunorubicin	DNA synthesis/topo II	6.60	7.30	6.98	7.03	7.66	6.88	6.79	7.55	7.17	7.98	7.18	7.74
Doxorubicin	DNA synthesis/topo II	6.39	7.45	6.79	6.71	7.32	6.70	6.39	7.14	6.86	7.87	6.68	7.66
Epirubicin	DNA synthesis/topo II	7.21	7.53	6.85	6.60	7.35	6.60	6.53	7.10	6.71	8.00	7.02	7.68
Mitoxantrone	DNA synthesis	6.82	7.52	6.57	6.52	7.79	6.68	6.87	7.82	6.83	8.79	7.38	7.59
Pirarubicin	DNA synthesis/topo II	8.31	8.97	8.55	8.57	9.00	8.53	8.81	9.00	8.56	9.00	8.86	9.00
Topotecan	Topo I	7.21	6.27	5.54	5.81	8.00	5.62	6.61	7.83	5.64	7.74	8.00	7.68
SN-38	Topo I	6.83	6.63	6.16	6.16	8.71	6.17	6.89	8.49	6.04	8.49	8.78	8.28
Camptothecin	Topo I	7.13	6.39	5.82	5.50	7.99	5.62	6.81	7.53	5.49	7.61	7.75	7.73
Bleomycin	DNA synthesis	4.00	4.61	4.03	4.00	4.54	4.22	4.00	6.21	4.22	7.18	6.03	4.75
Peplomycin	DNA synthesis	4.00	4.80	4.56	4.09	5.18	4.82	4.39	5.96	4.68	7.32	6.16	4.92
Neocarzinostatin	DNA synthesis	6.17	6.92	6.58	6.47	8.38	7.19	6.95	7.74	6.92	8.58	7.59	8.00
Irinotecan	Topo I	4.00	4.41	4.29	4.02	5.41	4.26	4.44	5.24	4.00	5.58	5.39	5.41
TAS103	Topo	5.75	7.54	6.50	6.56	7.50	6.43	6.96	7.97	6.81	8.51	7.40	7.76
Gemcitabine	Pyrimidine	4.09	6.17	4.45	4.00	8.00	5.38	6.18	7.57	4.00	8.00	6.68	7.70
Cladribine	Pyrimidine	4.11	4.51	4.00	4.00	6.88	4.00	4.00	5.56	4.00	6.52	4.43	5.42
Cytarabine	Pyrimidine	4.00	4.00	4.00	4.00	6.41	4.00	4.00	6.38	4.00	6.56	5.68	5.76
Etoposide	Topo II	4.67	5.79	4.59	4.51	5.43	4.22	4.96	5.55	5.22	6.23	5.80	5.90
Amsacrine	Topo II	5.30	6.24	5.01	4.96	6.43	5.34	5.75	6.55	5.50	6.98	6.44	6.68
2-Dimethylaminoetoposide	Topo II	4.70	5.63	4.57	4.37	5.67	4.29	4.97	5.75	5.05	5.99	5.72	6.14
NK109	Topo II	6.02	6.66	5.88	5.76	6.51	5.62	6.58	6.92	6.29	6.90	6.66	6.78
MMC	DNA alkylator	4.93	5.00	5.33	5.10	7.09	5.56	5.75	6.17	5.74	6.45	5.99	7.28
Methotrexate	DHFR	7.27	7.04	4.00	4.00	7.15	4.00	7.06	7.04	7.49	7.37	7.33	7.32
Radicicol	HSP90/Tyr kinase	6.96	6.59	5.88	5.66	6.44	6.15	6.40	6.89	6.00	6.63	7.42	6.08
Vinblastine	Tubulin	6.17	9.62	7.60	9.64	9.04	9.25	8.58	9.88	9.37	9.76	9.85	9.53
Vincristine	Tubulin	6.37	9.36	8.60	8.58	8.42	9.13	8.12	9.30	8.91	9.36	9.61	8.94
Vinorelbine	Tubulin	6.00	8.60	8.51	8.59	8.42	8.53	7.96	9.22	8.37	8.89	8.83	8.87
Paclitaxel	Tubulin	6.87	7.68	7.50	7.48	7.89	7.16	6.77	8.15	7.70	8.09	7.86	8.15
Docetaxel	Tubulin	7.05	8.06	8.10	8.32	8.47	7.71	6.93	8.85	8.19	9.08	8.50	8.51
Dolastatine 10	Tubulin	9.41	9.56	10.27	10.18	9.75	10.29	10.51	10.60	9.23	10.42	10.53	10.35
Colchicine	Tubulin	7.76	7.99	7.28	7.90	7.75	7.51	7.34	7.78	7.65	7.70	8.69	7.53
E7010	Tubulin	6.06	6.21	6.26	6.35	6.02	6.15	6.39	6.69	6.08	6.69	6.67	6.40
Melphalan	DNA cross-linker	4.47	4.70	4.19	4.00	4.79	4.36	4.55	4.59	4.72	5.18	5.26	5.32
Leptomycin B	Cell cycle inhibitor	9.45	9.44	9.36	9.25	9.45	9.50	9.15	9.48	9.57	9.81	9.69	9.54
Carboplatin	DNA cross-linker	4.00	4.25	4.00	4.00	4.00	4.00	4.00	4.14	4.00	4.00	4.24	4.97
Cisplatin	DNA cross-linker	4.78	5.61	5.07	4.66	5.47	4.48	5.35	5.46	4.75	5.12	5.60	6.52
4-Hydroperoxycyclo-phosphamide	DNA alkylator	4.37	4.77	4.81	4.92	5.13	4.76	4.85	4.81	4.80	5.30	5.25	5.33
6-Mercaptopurine	Purine	4.21	5.58	4.67	5.21	5.39	5.86	4.45	5.21	5.47	5.54	5.97	5.03
6-Thioguanine	Purine	6.18	6.13	5.49	5.46	5.66	5.74	5.83	5.57	5.83	6.21	6.53	5.36
L-Asparaginase	Protein synthesis	6.32	6.41	6.64	6.54	6.65	6.91	5.30	6.70	5.78	6.72	6.34	6.51
Estramustine	Estradiol	4.21	4.26	4.00	4.00	4.20	4.72	4.29	4.45	4.34	4.20	5.11	4.48
IFN-α	Biological response	4.00	4.00	4.00	4.00	4.00	4.51	4.00	4.00	4.00	4.00	4.00	4.00
IFN-β	Biological response	4.00	4.00	4.00	4.00	4.00	4.00	4.00	4.00	4.00	4.00	4.00	4.00
IFN-γ	Biological response	4.00	4.07	4.00	4.00	4.00	4.00	4.00	4.00	4.00	4.00	4.00	4.00

(Continued on the following page)

Table 1. The mode of actions and the median value of $|\log_{10}GI_{50}|$ of 53 anticancer drugs in each of the 45 cell lines (Cont'd)

Drug name	Target/ mode of action	Stomach								
		NUGC -3/5-FU	HSC-42	AGS	KWS-1	TGS-11	OKIBA	ISt-1	ALF	AOTO
Aclarubicin	DNA/RNA synthesis	7.51	8.21	8.27	7.96	8.31	7.20	7.19	8.54	7.57
Oxaliplatin	DNA cross-linker	5.23	5.98	5.58	6.26	7.02	5.85	5.14	5.46	4.78
Actinomycin D	RNA synthesis	8.56	9.32	8.99	9.22	9.55	9.35	8.77	9.39	8.88
HCFU	Pyrimidine	4.36	4.89	5.00	4.71	4.27	5.10	4.15	4.23	4.44
5-FU	Pyrimidine	4.00	4.40	5.02	4.50	4.06	6.38	4.00	4.42	4.09
Doxifluridine	Pyrimidine	4.00	4.00	4.26	4.00	4.00	4.18	4.00	4.00	4.00
E7070	Cell cycle inhibitor	4.39	4.81	4.46	5.25	4.96	6.05	4.83	6.69	4.97
Tamoxifen	Estrogen receptor	4.86	4.89	5.59	4.93	5.20	5.58	4.93	5.43	5.13
Toremifene	Estrogen receptor	4.85	4.88	5.00	4.93	5.07	5.58	4.88	5.50	5.24
MS-247	DNA synthesis	5.64	7.11	7.01	6.74	6.67	6.20	5.70	5.70	5.63
Daunorubicin	DNA synthesis/topo II	6.85	7.57	7.42	6.99	6.93	7.59	6.37	6.94	6.80
Doxorubicin	DNA synthesis/topo II	6.47	7.33	7.53	6.91	6.90	8.00	6.01	6.34	6.54
Epirubicin	DNA synthesis/topo II	6.13	7.61	8.02	7.12	6.91	7.12	5.99	7.00	6.51
Mitoxantrone	DNA synthesis	6.18	7.70	7.75	7.21	6.74	8.56	5.76	6.14	6.37
Pirarubicin	DNA synthesis/topo II	8.65	9.00	9.00	8.99	8.58	8.81	8.16	8.68	8.57
Topotecan	Topo I	5.82	8.00	7.54	6.07	6.39	6.10	6.70	6.90	6.85
SN-38	Topo I	6.31	8.61	8.70	6.81	6.66	7.07	7.29	7.46	7.28
Camptothecin	Topo I	6.00	7.76	7.23	6.36	6.64	6.81	6.43	6.72	6.96
Bleomycin	DNA synthesis	4.00	5.66	5.19	4.00	4.00	5.55	4.00	4.81	4.58
Peplomycin	DNA synthesis	4.05	6.00	5.82	4.65	4.08	5.92	4.23	5.04	4.78
Neocarzinostatin	DNA synthesis	6.54	7.89	7.78	6.84	6.60	7.05	6.54	6.74	7.24
Irinotecan	Topo I	4.06	5.48	5.50	4.25	4.58	4.64	4.42	4.56	4.71
TAS103	Topo	6.45	7.66	7.98	6.94	6.45	6.89	6.24	6.45	7.74
Gemcitabine	Pyrimidine	4.00	6.77	6.65	4.00	4.06	6.76	4.86	5.82	7.27
Cladribine	Pyrimidine	4.00	4.46	4.56	4.00	4.00	6.41	4.00	4.00	4.24
Cytarabine	Pyrimidine	4.00	5.96	5.60	4.00	4.00	7.32	4.00	5.58	4.00
Etoposide	Topo II	4.72	6.11	6.13	5.13	4.41	8.00	4.73	5.10	5.79
Amsacrine	Topo II	4.91	6.53	6.30	5.71	4.99	6.60	5.06	5.57	6.29
2-Dimethylaminoetoposide	Topo II	4.12	5.94	5.17	4.78	4.36	6.25	4.57	4.80	5.75
NK109	Topo II	5.95	6.70	6.47	6.63	5.68	7.27	5.79	5.91	6.86
MMC	DNA alkylator	5.58	6.27	6.23	5.86	5.75	5.56	5.32	6.03	5.86
Methotrexate	DHFR	4.00	7.38	7.53	7.81	4.00	6.66	4.00	4.00	4.00
Radicicol	HSP90/Tyr kinase	5.71	7.63	7.07	6.78	6.80	6.80	5.76	6.38	6.74
Vinblastine	Tubulin	8.20	9.85	9.69	9.80	9.28	9.71	7.04	8.12	8.33
Vincristine	Tubulin	7.12	9.70	9.24	9.35	9.41	10.00	6.00	7.46	8.20
Vinorelbine	Tubulin	7.13	9.32	8.86	8.87	8.58	9.79	6.00	8.25	8.64
Paclitaxel	Tubulin	6.49	8.07	7.74	7.96	8.03	8.29	6.52	7.79	7.52
Docetaxel	Tubulin	7.21	8.86	8.63	8.47	8.49	8.46	7.33	8.68	8.27
Dolastatine 10	Tubulin	8.89	10.69	10.50	10.44	10.13	11.86	8.69	10.09	10.26
Colchicine	Tubulin	5.98	8.59	8.19	8.34	7.45	8.74	6.05	7.56	7.84
E7010	Tubulin	4.37	6.69	6.47	6.64	6.27	6.88	4.51	5.50	5.36
Melphalan	DNA cross-linker	4.56	5.34	5.27	4.00	5.00	4.62	4.15	4.73	4.67
Leptomycin B	Cell cycle inhibitor	9.12	9.64	9.53	8.66	9.16	9.71	8.82	9.76	9.49
Carboplatin	DNA cross-linker	4.00	4.36	4.16	4.00	4.00	4.62	4.00	4.00	4.26
Cisplatin	DNA cross-linker	4.80	5.64	5.55	4.74	5.71	5.79	5.43	5.57	5.51
4-Hydroperoxycyclo-phosphamide	DNA alkylator	4.78	5.50	5.44	4.70	4.68	5.17	4.61	4.66	4.78
6-Mercaptopurine	Purine	5.19	5.90	5.86	4.95	4.55	4.85	4.00	4.00	4.00
6-Thioguanine	Purine	5.50	6.54	5.61	5.79	5.92	6.10	4.00	4.46	4.36
L-Asparaginase	Protein synthesis	6.63	6.47	6.93	6.51	4.94	6.52	4.00	5.56	4.00
Estramustine	Estradiol	4.08	5.03	4.74	4.42	4.02	4.79	4.59	4.95	4.76
IFN-α	Biological response	4.00	4.00	4.00	4.00	4.51	4.20	4.62	4.62	4.16
IFN-β	Biological response	4.00	4.00	4.00	4.00	6.02	4.93	4.77	6.28	6.54
IFN-γ	Biological response	4.00	4.00	4.00	4.00	4.00	4.00	4.00	5.06	4.00

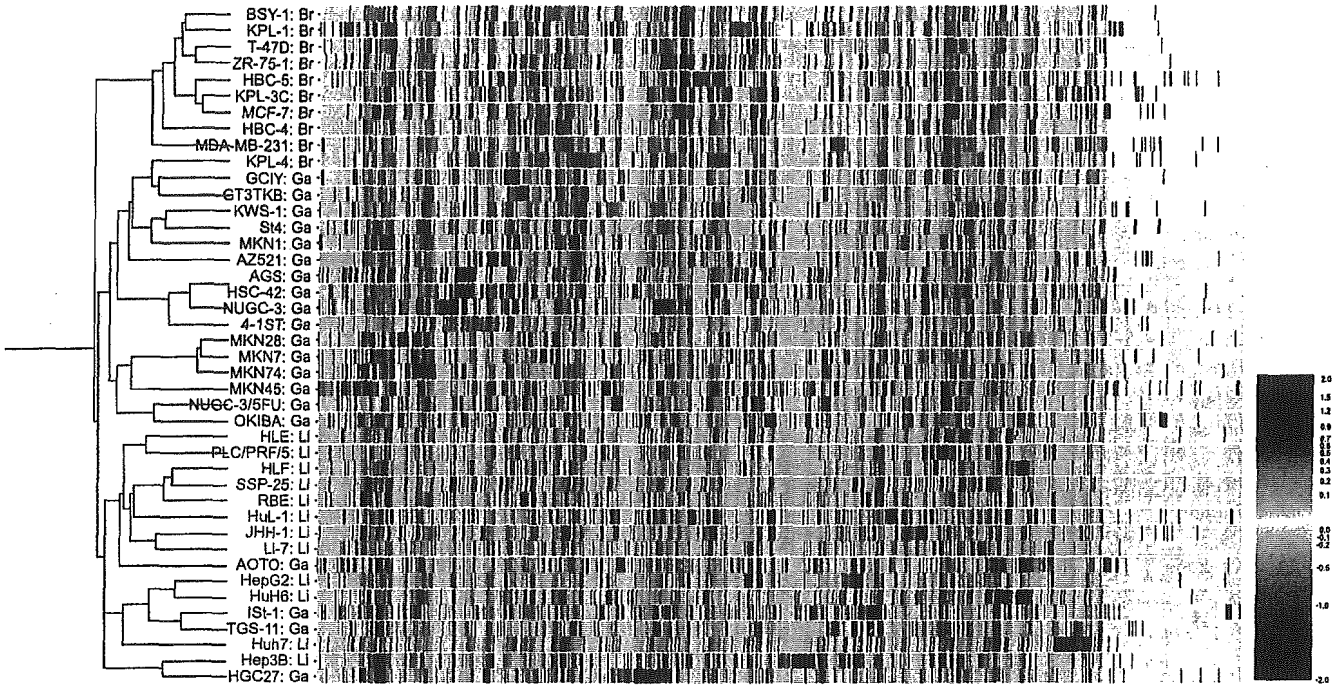

Figure 2. Hierarchical clustering of 42 human cancer cell lines based on their gene expression profiles. Gradient color indicates relative level (log_2 transformed) of gene expression. *Red,* high expression of gene (2.0); *yellow,* normal expression of gene (0.0); *green,* low expression of gene (−2.0). *Red* was expressed four times more than *yellow*. *Br*, *Ga*, and *Li,* breast, stomach, and liver cancer cell lines, respectively. Cell lines with the same tissue of origin tended to form a cluster.

cancer cell lines clustered separately from the breast cancer cell lines and formed tissue-specific subclusters. However, four stomach cancer cell lines, AOTO, ISt-1, TGS-11, and HGC27, were intercalated into a cluster of liver cancer cell lines. These results suggested that the established cell lines maintained characteristics of their organ of origin as far as the gene expression profile was concerned.

Correlation Analysis between Gene Expression Profiles and Chemosensitivity Profiles

To investigate genes that may be involved in chemosensitivity, we integrated the two databases and did a correlation analysis between gene expression and drug sensitivity. Comprehensive calculations for the Pearson correlation coefficients were done on the expression of 3,537 genes and sensitivity to 53 drugs in 42 cell lines. We selected genes that satisfied the following criteria: showing a P of correlation <0.05 between the expression of the gene and its sensitivity to a certain drug and being significantly expressed in >50% of the cell lines. We examined the data for the distribution by scatter graph analysis and removed those data showing a highly non-normal distribution. The higher the expression of the gene showing positive correlation, the higher the sensitivity was to the drug (i.e., this gene was a sensitive candidate gene). In contrast, genes that showed a negative correlation with chemosensitivity were resistant candidate genes. Consequently, different sets of genes were extracted with respect to each of the 53 drugs. Table 2 shows sets of genes whose expression was correlated with the sensitivity of 42 cell lines to MMC, paclitaxel, vinorelbine, and SN-38. As for MMC, 20 genes were extracted as sensitive genes and 10 genes were extracted as resistant candidate genes. Some of these genes (such as *JUN*, *EMS1*, and *NMBR*) are related to cell growth, whereas others included various types of genes (such as *SOD1*, *PELP1*, *SFRS9*, etc.). Similarly, many sensitive and resistant candidate genes were extracted with the other drugs tested. We further applied a Pearson correlation analysis to the cell lines originating from the same organ. Genes whose expressions were correlated with the MMC sensitivity in 10 breast cancer, 12 liver cancer, and 20 stomach cancer cell lines are shown in Table 3. As described previously (19, 20), these genes may predict chemosensitivity.

Identification of Genes That Change Cellular Chemosensitivity

These genes described above may include genes that directly determine chemosensitivity. To identify such genes, we established a screening system in which we could detect any change in the anticancer drug sensitivity by monitoring cell growth inhibition. [^{3}H]thymidine incorporation was used as a variable to measure cell growth. To detect small changes in sensitivity, a higher transfection efficiency was required. Therefore, the human fibrosarcoma cell line, HT1080, which reportedly showed high transfection efficiency, was selected for the subsequent experiments. Transfection efficiency of HT1080 cells

Table 2. Genes related to the sensitivity to MMC, vinorelbine, paclitaxel, and SN-38 in 42 human cancer cell lines

Rank	Gene	Genbank ID	r	P
A. MMC				
Sensitive				
1	*SF1*	D26121	0.566	0.001
2	*CBR3*	Ab004854	0.486	0.006
3	*EMS1*	M98343	0.480	0.010
4	*JUN*	J04111	0.473	0.015
5	*SFRS9*	U30825	0.448	0.010
6	*NMBR*	M73482	0.428	0.012
7	*RBMX*	Z23064	0.419	0.012
8	*SOD1*	M13267	0.418	0.024
9	*NOL1*	X55504	0.415	0.025
10	*PELP1*	U88153	0.405	0.019
11	*ARHA*	L25080	0.404	0.030
12	*AARS*	D32050	0.398	0.018
13	*NME1*	X17620	0.398	0.032
14	*HNRPA2B1*	M29065	0.390	0.044
15	*NME2*	L16785	0.378	0.025
16	*VAT1*	U18009	0.376	0.031
17	*SERPINB10*	U35459	0.372	0.028
18	*KIAA0436*	AB007896	0.353	0.041
19	*DRPLA*	D31840	0.350	0.049
20	*MC3R*	L06155	0.346	0.049
Resistant				
1	*SPTBN1*	M96803	−0.450	0.013
2	*PET112L*	AF026851	−0.425	0.027
3	*CAPN1*	X04366	−0.421	0.032
4	*MEL*	X56741	−0.414	0.028
5	*PACE*	X17094	−0.380	0.035
6	*DVL2*	AF006012	−0.370	0.034
7	*LOC54543*	AJ011007	−0.366	0.022
8	*PAPOLA*	X76770	−0.351	0.033
9	*RPLP2*	M17887	−0.345	0.049
10	*ARF4L*	L38490	−0.340	0.042
B. Vinorelbine				
Sensitive				
1	*ARHA*	L25080	0.534	0.003
2	*NME2*	L16785	0.521	0.001
3	*VIL2*	X51521	0.463	0.015
4	*YWHAQ*	X56468	0.450	0.011
5	*HK1*	M75126	0.449	0.016
6	*SATB1*	M97287	0.439	0.006
7	*CAMLG*	U18242	0.439	0.007
8	*CARS*	L06845	0.433	0.007
9	*CCNB1*	M25753	0.427	0.013
10	*U2AF1*	M96982	0.424	0.022
11	*PTMA*	M26708	0.423	0.018
12	*MLC1SA*	M31211	0.397	0.022
13	*NME1*	X17620	0.393	0.035
14	*SARS*	X91257	0.386	0.032
15	*CDC20*	U05340	0.385	0.029
16	*PPP4C*	X70218	0.385	0.039
17	*TNFAIP3*	M59465	0.384	0.023
18	*EEF1D*	Z21507	0.384	0.023
19	*PFKP*	D25328	0.365	0.028
20	*ENTPD2*	U91510	0.365	0.037
21	*CCL5*	M21121	0.358	0.035
22	*ACAT1*	D90228	0.352	0.048
23	*IQGAP1*	L33075	0.351	0.042
24	*PAX5*	M96944	0.342	0.038
25	*NRGN*	Y09689	0.336	0.042
26	*K-α-1*	K00558	0.328	0.048
27	*NDUFB7*	M33374	0.321	0.049
Resistant				
1	*HOXB1*	X16666	−0.600	0.000
2	*F10*	K03194	−0.514	0.002
3	*GPX2*	X53463	−0.509	0.002
4	*NR1I2*	AF061056	−0.498	0.002
5	*ANXA4*	M19383	−0.481	0.005
6	*PDLIM1*	U90878	−0.465	0.006
7	*LIPC*	X07228	−0.464	0.004
8	*SERPINF2*	D00174	−0.447	0.004
9	*HSD17B1*	M36263	−0.443	0.014
10	*MAN2B1*	U60266	−0.440	0.008
11	*LSS*	D63807	−0.430	0.014
12	*PIK3CG*	X83368	−0.415	0.010
13	*DBN1*	U00802	−0.414	0.017
14	*NDUFA4*	U94586	−0.410	0.038
15	*BDH*	M93107	−0.399	0.024
16	*BCL2L1*	Z23115	−0.385	0.039
17	*EEF1B2*	X60656	−0.383	0.030
18	*F2*	V00595	−0.382	0.026
19	*RARA*	X06614	−0.369	0.029
20	*ITGB4*	X53587	−0.367	0.042
21	*IMPA1*	X66922	−0.367	0.042
22	*PACE*	X17094	−0.367	0.042
23	*AGA*	M64073	−0.361	0.042
24	*MVD*	U49260	−0.353	0.038
25	*EHHADH*	L07077	−0.346	0.039
26	*TFPI2*	D29992	−0.343	0.035
27	*MARCKS*	M68956	−0.342	0.045
28	*FGB*	J00129	−0.334	0.035
29	*GPD1*	L34041	−0.322	0.049
C. Paclitaxel				
Sensitive				
1	*ADH6*	M68895	0.513	0.002
2	*RAB28*	X94703	0.480	0.007
3	*U2AF1*	M96982	0.441	0.017
4	*GPC1*	X54232	0.440	0.013
5	*HK1*	M75126	0.439	0.020
6	*CARS*	L06845	0.436	0.006
7	*TNFAIP3*	M59465	0.433	0.009
8	*K-α-1*	K00558	0.418	0.010
9	*PFKP*	D25328	0.416	0.012
10	*GDI2*	D13988	0.411	0.033
11	*VIL2*	X51521	0.410	0.034
12	*RUNX2*	AF001450	0.409	0.038
13	*NME2*	L16785	0.407	0.015
14	*CDC20*	U05340	0.395	0.025
15	*GNAI2*	X04828	0.391	0.033

NOTE: Column 2 shows the name of the gene according to HUGO database. Column 4 shows Pearson correlation coefficient between chemosensitivity to drugs and gene expression. "Sensitive" indicates candidate genes sensitive to each drug. "Resistant" indicates genes resistant to each drug.

(Continued on the following page)

Table 2. Genes related to the sensitivity to MMC, vinorelbine, paclitaxel, and SN-38 in 42 human cancer cell lines (Cont'd)

Rank	Gene	Genbank ID	*r*	*P*
16	*ARHA*	L25080	0.381	0.041
17	*CNR2*	X74328	0.378	0.030
18	*PPP2R2B*	M64930	0.376	0.026
19	*SLC6A8*	L31409	0.374	0.046
20	*DDX9*	L13848	0.374	0.042
21	*ACAT1*	D90228	0.369	0.038
22	*PI3*	Z18538	0.329	0.047
Resistant				
1	*NAP1L1*	M86667	−0.530	0.004
2	*HOXB1*	X16666	−0.516	0.004
3	*PACE*	X17094	−0.507	0.004
4	*MAN2B1*	U60266	−0.486	0.003
5	*GPX2*	X53463	−0.480	0.004
6	*DBN1*	U00802	−0.469	0.006
7	*ANXA4*	M19383	−0.468	0.007
8	*SERPINF2*	D00174	−0.463	0.003
9	*AGA*	M64073	−0.444	0.011
10	*BCL2L1*	Z23115	−0.428	0.021
11	*LIPC*	X07228	−0.401	0.015
12	*BDH*	M93107	−0.393	0.026
13	*LSS*	D63807	−0.384	0.030
14	*PDLIM1*	U90878	−0.372	0.033
15	*ZNF161*	D28118	−0.368	0.038
16	*UBE2E1*	X92963	−0.363	0.032
17	*TLE1*	M99435	−0.360	0.039
18	*RARA*	X06614	−0.359	0.034
19	*PTPRN*	L18983	−0.357	0.035
20	*APOE*	M12529	−0.353	0.048
21	*F10*	K03194	−0.348	0.040
22	*NR1I2*	AF061056	−0.342	0.041
23	*UBE2L3*	X92962	−0.332	0.045
24	*FGB*	J00129	−0.313	0.049
D. SN-38				
Sensitive				
1	*EMS1*	M98343	0.573	0.001
2	*JUN*	J04111	0.564	0.003
3	*IL-6*	X04602	0.514	0.003
4	*RPL23*	X52839	0.495	0.004
5	*CDKN3*	L25876	0.455	0.017
6	*RPL3*	X73460	0.445	0.011
7	*TFPI*	J03225	0.442	0.009
8	*MRPL3*	X06323	0.437	0.009
9	*HLA-C*	M11886	0.424	0.014
10	*AARS*	D32050	0.419	0.012
11	*ARHGDIA*	X69550	0.416	0.031
12	*NOL1*	X55504	0.406	0.029
13	*SF1*	D26121	0.394	0.031
14	*SOD1*	M13267	0.389	0.037
15	*VEGF*	M32977	0.384	0.043
16	*EIF2S1*	J02645	0.382	0.034
17	*CDH5*	X79981	0.372	0.030
18	*FOSL1*	X16707	0.371	0.047
19	*IDS*	M58342	0.366	0.047
20	*PMVK*	L77213	0.364	0.044
21	*PPP2CB*	X12656	0.364	0.041
22	*NMBR*	M73482	0.362	0.035
23	*RPL26*	X69392	0.358	0.035
24	*PELP1*	U88153	0.356	0.042
25	*MC3R*	L06155	0.356	0.042
26	*RPS8*	X67247	0.355	0.036
Resistant				
1	*CAPN1*	X04366	−0.496	0.010
2	*MEL*	X56741	−0.478	0.010
3	*PACE*	X17094	−0.443	0.012
4	*TIMP2*	J05593	−0.433	0.019
5	*AOP2*	D14662	−0.422	0.025
6	*ZNF174*	U31248	−0.402	0.018
7	*ID3*	X69111	−0.393	0.038
8	*KLF5*	D14520	−0.384	0.036
9	*CALD1*	M64110	−0.382	0.031
10	*LOC54543*	AJ011007	−0.368	0.021
11	*PTPN3*	M64572	−0.363	0.038
12	*ACTB*	X00351	−0.362	0.025
13	*LY6E*	U42376	−0.360	0.037
14	*ID1*	D13889	−0.343	0.044

(Continued)

was >90% as evaluated by transfection of a plasmid expressing the enhanced green fluorescent protein (data not shown). To validate this screening system, we examined the effect of *NQO1* gene, coding DT-diaphorase that increases cellular sensitivity to MMC (12). As shown in Fig. 3B, cells transfected with NQO1 significantly enhanced growth inhibition by MMC compared with the mock-transfected and LacZ-transfected cells. We confirmed the cellular expression of the *NQO1* gene product by immunoblot (Fig. 3C). Thus, this screening system can be used to detect changes in chemosensitivity in HT1080 cells. Using this screening system, we examined whether the 19 genes, which were extracted in Tables 2 and 3, altered sensitivity to drug. Notably, the *HSPA1A* gene coding 70-kDa heat shock protein, whose expression was correlated with MMC sensitivity in the breast and liver cancer cell lines, significantly enhanced the MMC sensitivity in HSPA1A-transfected HT1080 cells (Fig. 3B). Similarly, the *JUN* gene encoding c-JUN, whose expression was correlated with MMC sensitivity, also enhanced the MMC sensitivity in JUN-transfected HT1080 cells (Fig. 3B). The expression of *myc*-tagged LacZ, 70-kDa heat shock protein, and JUN in the transfected cells was confirmed by immunoblotting with anti-*myc* antibody (Fig. 3C). Transfection with 17 other genes did not alter the MMC sensitivity. For example, transfection with the *IL-18* gene did not affect MMC sensitivity (Fig. 3B).

Discussion

The assessment system for determining pharmacologic properties of chemicals by a panel of cancer cell lines was first developed in the National Cancer Institute (33–35). We established a similar assessment system (JFCR-39;

Table 3. Genes related to MMC sensitivity in breast, liver, and stomach cancer cell lines

Rank	Gene	Genbank ID	*r*	*P*
A. Breast cancer				
Sensitive				
1	*INHBB*	M31682	0.972	0.000
2	*NK4*	M59807	0.838	0.018
3	*HSPA1A*	M11717	0.751	0.050
4	*LOC54557*	AF075050	0.735	0.024
5	*CD47*	Y00815	0.717	0.045
Resistant				
1	*RPN2*	Y00282	−0.882	0.009
2	*ATP5O*	X83218	−0.842	0.017
3	*CAST*	D50827	−0.815	0.025
4	*HPCA*	D16593	−0.776	0.024
5	*ZNF9*	M28372	−0.774	0.024
6	*A2LP*	U70671	−0.772	0.042
7	*IL-18*	D49950	−0.747	0.033
8	*NRGN*	Y09689	−0.727	0.041
B. Liver cancer				
Sensitive				
1	*EB1*	U24166	0.872	0.002
2	*JUN*	J04111	0.813	0.008
3	*EIF3S8*	U46025	0.772	0.015
4	*CTSD*	M11233	0.753	0.012
5	*SCYA5*	M21121	0.741	0.022
6	*PHB*	S85655	0.739	0.023
7	*HSPA1A*	M11717	0.729	0.026
8	*SPP1*	X13694	0.723	0.018
9	*TAB7*	X93499	0.712	0.021
10	*ACTN1*	X15804	0.692	0.039
11	*RXRB*	M84820	0.678	0.045
12	*PSME2*	D45248	0.673	0.047
13	*HLA-C*	M11886	0.647	0.043
14	*RPL19*	X63527	0.643	0.033
Resistant				
1	*MAPK6*	X80692	−0.862	0.003
2	*GCSH*	M69175	−0.793	0.006
3	*G22P1*	M32865	−0.727	0.017
4	*USP11*	U44839	−0.725	0.027
5	*ACTB*	X00351	−0.715	0.020
6	*YWHAZ*	M86400	−0.706	0.022
7	*IL-10*	M57627	−0.694	0.018
8	*RFC4*	M87339	−0.677	0.016
9	*CRLF1*	AF059293	−0.644	0.033
10	*RPS6*	M20020	−0.619	0.042
11	*EMX1*	X68879	−0.618	0.043
12	*TK2*	U77088	−0.607	0.047
C. Stomach cancer				
Sensitive				
1	*TEAD4*	U63824	0.803	0.001
2	*NR2C2*	U10990	0.713	0.001
3	*CSF1*	M37435	0.711	0.004
4	*RAB28*	X94703	0.695	0.008
5	*CBR3*	Ab004854	0.683	0.007
6	*NFYC*	Z74792	0.639	0.019
7	*PGF*	X54936	0.627	0.022
8	*ERG*	M21535	0.620	0.005
9	*MLLT1*	L04285	0.613	0.015
10	*FOS*	K00650	0.599	0.014
11	*TNFAIP3*	M59465	0.584	0.011
12	*CNR2*	X74328	0.581	0.009
13	*DRPLA*	D31840	0.577	0.024
14	*PSMB5*	D29011	0.572	0.026
15	*SLC6A8*	L31409	0.570	0.017
16	*SERPINB10*	U35459	0.570	0.013
17	*VAT1*	U18009	0.570	0.009
18	*TJP1*	L14837	0.562	0.029
19	*PELP1*	U88153	0.545	0.035
20	*C1QBP*	L04636	0.545	0.024
21	*CDK10*	L33264	0.543	0.045
22	*SERPINA6*	J02943	0.542	0.025
23	*ACTB*	X00351	0.538	0.021
24	*SFRP4*	AF026692	0.538	0.018
25	*EMX1*	X68879	0.535	0.018
26	*ACTB*	X00351	0.529	0.024
27	*RPS9*	U14971	0.528	0.043
28	*AMD1*	M21154	0.522	0.038
29	*RPL26*	X69392	0.522	0.038
30	*HNRPF*	L28010	0.520	0.047
31	*PTMS*	M24398	0.502	0.040
32	*STK12*	AF008552	0.498	0.050
33	*NR2F6*	X12794	0.491	0.046
34	*GBE1*	L07956	0.470	0.049
Resistant				
1	*PSMD8*	D38047	−0.747	0.002
2	*LAMP2*	J04183	−0.677	0.002
3	*CTSD*	M11233	−0.651	0.006
4	*ADORA2B*	M97759	−0.645	0.005
5	*ANXA4*	M19383	−0.639	0.008
6	*PTPRK*	Z70660	−0.638	0.003
7	*RAD23A*	D21235	−0.622	0.010
8	*SDHA*	D30648	−0.613	0.015
9	*PET112L*	AF026851	−0.598	0.024
10	*DAD1*	D15057	−0.593	0.025
11	*HSPB1*	X54079	−0.588	0.013
12	*PSMA6*	X61972	−0.586	0.036
13	*KDELR1*	X55885	−0.584	0.028
14	*B2M*	AB021288	−0.581	0.023
15	*M6PR*	M16985	−0.579	0.038
16	*GCLC*	M90656	−0.576	0.015
17	*SPTBN1*	M96803	−0.557	0.038
18	*PACE*	X17094	−0.547	0.019
19	*RPL24*	M94314	−0.539	0.017
20	*SPINT2*	U78095	−0.538	0.039
21	*STX4A*	U07158	−0.534	0.027
22	*SIAT8B*	U33551	−0.532	0.028
23	*CTSK*	U13665	−0.529	0.029
24	*DCI*	L24774	−0.525	0.044
25	*MEL*	X56741	−0.525	0.045
26	*PITPNB*	D30037	−0.523	0.038
27	*YY1*	M76541	−0.512	0.043
28	*RAB1*	M28209	−0.495	0.037
29	*UBE2L6*	AF031141	−0.492	0.045
30	*PSMB7*	D38048	−0.484	0.049

NOTE: Column 2 shows the name of the gene according to HUGO database. Column 4 shows Pearson correlation coefficient between chemosensitivity to drugs and gene expression. "Sensitive" indicates candidate genes sensitive to each drug. "Resistant" indicates genes resistant to each drug.